A Second-Generation Blackbody System for the Calibration and Verification of Seagoing Infrared Radiometers

CRAIG J. DONLON

European Space Agency, Noordwijk, Netherlands

W. WIMMER, I. ROBINSON, AND G. FISHER

National Oceanography Centre, University of Southampton, Southampton, United Kingdom

M. FERLET AND T. NIGHTINGALE

Space Science and Technology Department, Rutherford Appleton Laboratory, Didcot, United Kingdom

B. BRAS

European Space Agency, Noordwijk, Netherlands

(Manuscript received 17 July 2013, in final form 13 December 2013)

ABSTRACT

Quasi-operational shipborne radiometers provide a fiducial reference measurement (FRM) for satellite validation of satellite sea surface skin temperature (SST_{skin}) retrievals. External reference blackbodies are required to verify the performance and to quantify the accuracy of the radiometer calibration system. They provide a link in an unbroken chain of comparisons between the shipborne radiometer and a traceable reference standard. A second-generation water bath blackbody reference radiance source has been developed for this purpose. The second generation Concerted Action for the Study of the Ocean Thermal Skin (CASOTS-II) blackbody has a 110-mm-diameter aperture cylinder-cone geometry coated with NEXTEL suede 3103 paint. Interchangeable aperture stops reduce the cavity aperture diameter and minimize stray radiation. Monte Carlo modeling techniques show the effective emissivity of the cavity to be >0.9999 (aperture < 30 mm). The cavity is immersed in a water bath that is vigorously stirred using a pump that slowly heats the water bath at a mean rate of $\sim 0.6\,K\,h^{-1}$. The temperature of the water bath is measured using a thermometer traceable to the International System of Units (SI) standards. The worst-case radiance temperature of the CASOTS-II blackbody system is traceable to the SI with an uncertainty of 58 mK (millikelvin). When operating under typical laboratory conditions using an aperture of 40 mm, the uncertainty is 16 mK. An intercomparison with the U.K. National Physical Laboratory Absolute Measurements of Blackbody Emitted Radiance (AMBER) reference radiometer found no significant differences within 75 mK (110-mm aperture) or 50 mK (40-mm aperture), which is the combined uncertainty of the comparison and the reference standard for SI traceability of ISAR radiometer SST_{skin} records used for satellite SST validation. Applications of the CASOTS-II blackbody to monitor the calibration of shipborne radiometers are described and measurement protocols are proposed.

1. Introduction

The Copernicus program is a joint initiative of the European Commission (EC) and the European Space Agency (ESA) to establish a European capacity for Earth observation. Copernicus is designed to provide European policy makers and public authorities with accurate and timely information to better manage the environment, to understand and mitigate the effects of climate change, and to ensure civil security. The Sentinel-3 satellite (Donlon et al. 2012) carries the Sea and Land Surface Temperature Radiometer (SLSTR; see Coppo et al. 2010) that will provide state-of-the art dual-view sea surface temperature (SST), land surface temperature (LST), and ice surface temperature (IST) measurements over

Denotes Open Access content.

Corresponding author address: Craig J. Donlon, European Space Agency, Keplerlaan 1, 2201 AG Noordwijk, Netherlands.
E-mail: craig.donlon@esa.int

DOI: 10.1175/JTECH-D-13-00151.1

the earth's surface in support of Copernicus services (e.g., Bahurel et al. 2010). Reliable estimates of uncertainty must be attached to all SST, LST, and IST satellite data (e.g., Donlon et al. 2007) for use in data assimilation schemes and to verify the quality of the satellite measurements. In addition, rigorous methods are being developed (Merchant et al. 2012) to derive high-quality satellite SST as an essential climate variable (ECV) that must also be validated using independent measurements traceable to international standards. Part of the process for achieving this goal is the end-to-end validation of satellite-derived products using accurate and independent in situ reference measurements as part of a comprehensive validation strategy.

The Group for High Resolution SST (GHRSST) has fostered the development of new global SST data products based on the complementary characteristics of diverse types of SST observing systems (e.g., Donlon et al. 2007, 2009), which include uncertainty estimates derived largely from the global drifting buoy array (e.g., Meldrum et al. 2010). While these estimates of uncertainty are robust in an operational sense, the quality of in situ drifter measurements cannot easily be verified once a drifter is deployed at sea. A new approach has been developed over the last 10 years using a new generation of shipborne in situ infrared radiometer systems (e.g., Minnett et al. 2001; Jessup et al. 2002; Donlon et al. 2008) that measure the radiometric skin temperature (SST_{skin}) of the ocean surface. Shipborne radiometer measurements of SST_{skin} are complementary to the drifting buoy subsurface SST measurements because they allow a more direct validation of SST derived from satellite infrared radiometry: shipborne SST_{skin} is the same quantity that is measured by a satellite infrared radiometer after compensating for the impacts of the atmosphere; and shipborne SST_{skin} measurements eliminate uncertainties related to the near-surface ocean thermal structure that complicates comparisons between subsurface thermometry and satellite observations of SST_{skin}. Furthermore, the internal calibration of shipborne radiometers can be verified before and after each deployment in a manner that is traceable to national temperature standards.

Since 2004 10 Infrared Sea Surface Autonomous Radiometers (ISARs; Donlon et al. 2008) have been manufactured for use in satellite validation and other studies. They rely on internal blackbody calibration targets and maintain a measurement accuracy of ± 0.1 K. These instruments have collected extensive validation datasets in different regions by different groups (e.g., Noyes et al. 2006), including SST validation in the China Sea (Guan et al. 2011), the Atlantic and Pacific Oceans (Minnett 2010), the English Channel, and the Bay of Biscay (Wimmer et al. 2012). In addition to SST validation activities, radiometers have been used to validate satellite IST over Greenland sea ice (e.g., Dybkjær et al. 2012) and LST (e.g., Coll et al. 2011). In situ temperature datasets obtained from radiometers such as ISAR provide one underpinning element of the SST, IST, and LST climate data records (CDR).

To ensure that Sentinel-3 SLSTR and other satellite-derived SST, IST, and LST measurements are traceable to the International System of Units (SI) standards and to satisfy the guidelines of the Global Climate Observing System (GCOS Secretariat 2009, 2011), ground-based radiometer measurements used for validation experiments must themselves be validated regularly against traceable radiometric standards (Minnett and Corlett 2012). In this context, shipborne radiometers provide a fiducial reference measurement (FRM) for satellite validation activities. This is considered mandatory for the validation of the Sentinel-3 SLSTR (Donlon et al. 2012), which is expected to begin operations in 2015.

The Concerted Action for the Study of the Ocean Thermal Skin (CASOTS) program specifically developed a CASOTS-I low-cost, portable reference blackbody to perform laboratory calibrations of shipborne radiometers before, during, and after ship deployments (Donlon et al. 1999). This paper describes a new CASOTS-II reference blackbody that was developed to replace the CASOTS-I unit. The new unit addresses minor shortcomings in the original CASOTS-I design in order to improve both the radiance characteristics and the ease of use. Section 2 of the paper identifies the design requirements of the CASOTS-II blackbody, section 3 explains the new design, and section 4 assesses its performance, leading to an uncertainty estimate for the end-to-end CASOTS-II system. It also includes results from a recent international reference blackbody intercomparison experiment. Section 5 describes how the CASOTS-II was used to quality control datasets of skin SST acquired from ISARs over 9 yr of satellite SST validation work. Part 6 distills this experience into a set of protocols for validating shipborne radiometers.

2. Second-generation CASOTS-II blackbody design requirements

Donlon et al. (1999) initially set out the requirements for the original CASOTS-I water bath blackbody as follows:

- The blackbody cavity shall have a large aperture that can accommodate a range of different radiometer fields of view.
- The blackbody cavity shall operate over a temperature range similar to that expected for global SST.

- The emissivity (ε) of the cavity shall be >0.99 in the 8–14-μm spectral wave band.
- The cavity temperature shall be accurately and reliably determined.
- Temperature gradients within the cavity shall be minimal.
- The blackbody unit shall be portable and be capable of operating in the field.

The first CASOTS-I design to meet these requirements was a cylinder–cone arrangement developed from an analysis of different geometric configurations that have high effective emissivity for a large range of spot radii [i.e., the field of view (FoV) radius of a radiometer falling on the reference blackbody surface when viewing along the axis of the reference blackbody]. The CASOTS-I design maintained high emissivity at spot radii up to 40 mm and was manufactured from a single sheet of copper spun over a steel mandrel and painted on all internal surfaces using NEXTEL velvet coating 811-21 (Lohrengel and Todtenhaupt 1996). The cavity was mounted in a water bath that was vigorously stirred by an immersed water pump. The temperature of the water bath was monitored using a precision platinum resistance thermometer. By design, the water pump self-heated the water bath at a mean rate of $\sim$0.2 K min^{-1} (defined by the specific pump thermal input, pump capacity characteristics, and heat-loss characteristics of the water bath). This allowed laboratory validation measurements of shipborne radiometers to be collected over a slowly varying range of temperature rather than at fixed set-point temperatures.

During the Committee on Earth Observation Satellites (CEOS) in situ radiometer intercalibration workshop (Kannenberg 1998), the CASOTS-I system demonstrated radiometric temperatures accurate to $\pm$0.02 K (Donlon et al. 1999) using Marine-Atmospheric Emitted Radiance Interferometer (M-AERI; Minnett et al. 2001) as a transfer radiometer when compared to a National Institute of Standards and Technology (NIST) blackbody unit (Geist and Fowler 1986; Fowler 1995). The CASOTS-I design was among several infrared blackbody sources evaluated in a second intercalibration exercise at the University of Miami in 2001. The brightness temperatures of different blackbodies were compared using the NIST Thermal Infrared Transfer Radiometer (TXR; see Rice et al. 2004). Although the resulting uncertainty did not exceed the $\pm$0.1-K design target when using the CASOTS-I source for calibrating shipborne radiometers, this was still considered too large an error to be acceptable within the validation procedures for climate-quality SST datasets.

A critical examination of CASOTS-I system performance in light of the limitations identified by Rice et al. (2004) pointed to elements in the design where improvements were required as follows:

- An improved radiance cavity design was required to accommodate the larger FoV of the ISAR radiometer (full-width beam divergence of 6°) and to improve its effective emissivity.
- There was a need for aperture stops of different sizes that could match the radiance cavity aperture to different radiometer FoV and enable improved cavity effective emissivity at smaller apertures (e.g., Berry 1981).
- An improved radiance cavity mounting arrangement within the water bath was required to minimize unacceptable thermal gradients at the cavity aperture edge.
- A removable cover to protect the radiance cavity surfaces when not in use was needed (this was not easy to implement for the CASOTS-I due to the design of the radiance cavity).
- Uncertainty in the homogeneity of the CASOTS-I radiance cavity wall thickness due to the spun-copper manufacture process was unknown.
- There was a need to improve the water bath insulation properties and water pump heating characteristics to reduce the internal heating rate of the water bath.
- An increase of the water pump flow capacity was desirable to maintain better temperature uniformity within the water bath and across the internal surface of the cavity over an ISAR radiometer measurement cycle.
- The cost of manufacture was to be reduced to encourage other shipborne radiometer users to acquire their own reference blackbody and to improve the quality of their measurement dataset.

In response, a new CASOTS-II blackbody reference cavity was designed specifically for the ISAR radiometer system used at the University of Southampton, but with sufficient flexibility to adapt to other radiometers.

3. CASOTS-II blackbody system design

The CASOTS-II blackbody system design follows the same overall principles as for the CASOTS-I system, in which a blackbody cavity is immersed in a vigorously stirred water bath that is heated by a high-volume water pump immersed in the bath. A precision reference thermometer traceable to SI standards measures the water bath temperature. After accounting for cavity emissivity and thermal gradients across the cavity wall and paint, the measured water bath temperature is related to the radiant temperature of the cavity. By design, there is no direct temperature control of the water bath

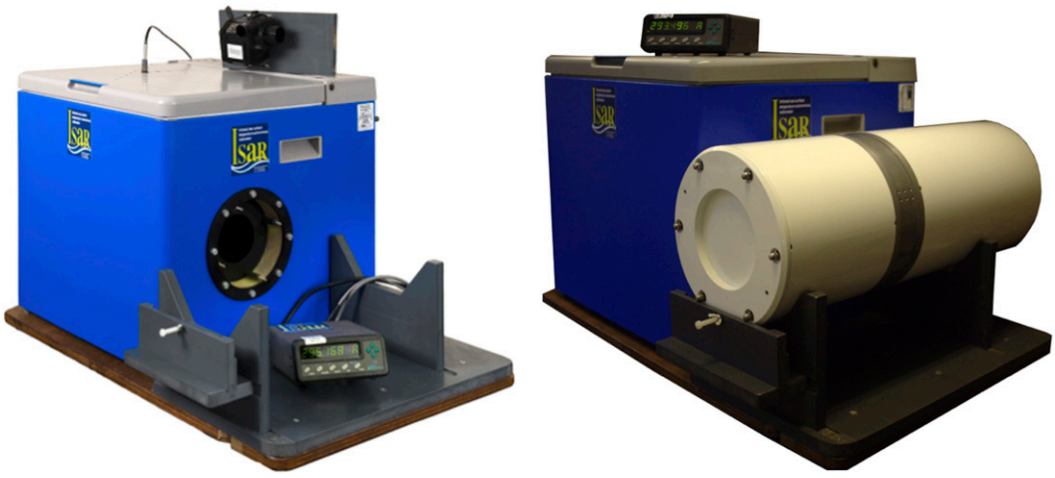

FIG. 1. CASOTS-II blackbody system with aperture protection plate removed from the protruding studs. (left) The ISAR radiometer mounting jig is shown in front of the circular aperture with the Hart Scientific 1504 bridge. A Thermometrics temperature probe 225 is shown at the top protruding from the water bath lid and the water bath pump (fitted internally when the unit is in operation) is also shown on top of the lid. (right) The CASOTS-II blackbody system showing an ISAR radiometer mounted for calibration verification.

to stabilize the water bath at a set temperature. This approach has been used successfully for many years within the ISAR program. Set-temperature water baths are available with excellent performance (e.g., Fowler 1995), but they are expensive and also violate the CASOTS-II design requirements. An external view of the new CASOTS-II blackbody system is shown in Fig. 1.

To ensure exact repeatability of ISAR calibration verification, a cradle was designed for the ISAR radiometer that guarantees the ISAR aperture is aligned exactly with the center of the CASOTS-II blackbody aperture. The vertical alignment of an ISAR radiometer can be finely adjusted using set screws and radially aligned using location screws that ensure the ISAR is horizontal relative to the CASOTS-II cavity axis. The CASOTS-II is fixed to the cradle baseplate to ensure that it does not move in relation to the instrument cradle. Once the cradle is set up, it is easy to interchange ISAR radiometers, secure in the knowledge that the alignment is identical. The CASOTS-II system can be dismantled for field experiments and fits into a standard aluminum crate for secure and easy transportation.

We note here that our primary application is to maintain the traceable calibration of ISAR shipborne radiometers that measure the SST_{skin} temperature. This application requires that the radiant temperature of the atmosphere is also measured which, in cloud-free conditions, can be very low (120–270 K, primarily depending on the water vapor content and its vertical distribution). Consequently, our blackbody design should ideally allow the calibration of our radiometer at these low temperatures. However, this is a challenge. The CASOTS-II design, like all other blackbody reference radiance sources that do not include a dry air (e.g., nitrogen) purge system, is not capable of operating below local dewpoint temperatures. Care must be taken not to select water bath temperatures below the local dewpoint temperature to avoid condensation forming on the blackbody cavity surfaces and thus decoupling the water bath temperature from the radiant temperature of the blackbody cavity due to thermal skin temperature gradients in the condensate layer. Developing such a capability is extremely challenging due to the effects of ice buildup on the blackbody, rendering it useless as a reliable calibration radiance source. Specialized equipment is required to ensure a completely dry atmosphere in addition to specialized materials that can withstand such cold temperatures, both of which are beyond the resources and scope of the present blackbody design reported here. Furthermore, we note that several other blackbody systems used by standards agencies are also unable to accommodate this aspect.

a. Water bath design

The CASOTS-II water bath design uses a larger water bath with significantly better insulation properties than the original CASOTS-I design. A Hozelock Cascade 4000 LV pump (24-V ac) is mounted within the water bath so that the pump outflow water jet flows underneath the cavity toward the front of the water bath, where it flows up and then recirculates along the cavity axis. This arrangement was selected following extensive tests of different water pump locations. The pump has

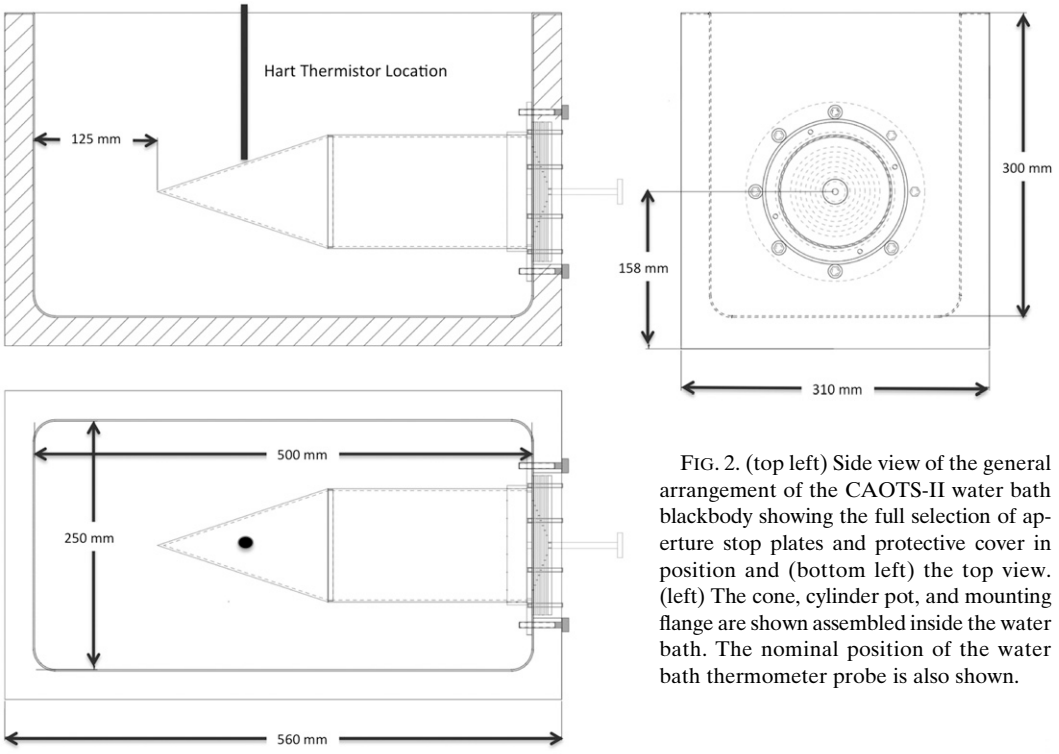

FIG. 2. (top left) Side view of the general arrangement of the CAOTS-II water bath blackbody showing the full selection of aperture stop plates and protective cover in position and (bottom left) the top view. (left) The cone, cylinder pot, and mounting flange are shown assembled inside the water bath. The nominal position of the water bath thermometer probe is also shown.

a 4000 L h^{-1} (~1.0 L s^{-1}) capacity that ensures that the water bath is well mixed at all times. In addition, the pump provides thermal input to warm the water bath at a very slow rate.

When higher blackbody reference temperatures are required above 320 K (e.g., for radiometers used to validate satellite LST retrievals where surface temperatures may be significantly higher than for SST), small heaters have been used to slowly increase the water bath temperature. The CASOTS-II water bath is not intended for use with synthetic oils that are used to reach temperatures above 373 K, as in some blackbody designs (Fowler 1996).

b. *Cavity geometry and manufacture*

The CASOTS-II cavity was redesigned following a modified version of the cylindrical tube and cone blackbody cavity designed by Fowler (1995) in which the cylinder length is extended to be greater than the cone height. A general arrangement of the CASOTS-II cavity design is shown in Fig. 2. The cavity is manufactured as three separate components from turned aluminum: a water bath mounting flange; a 110-mm internal diameter, 200-mm-long cylinder section; and a 170-mm-long cone section. The three components are manufactured to ensure a water-tight interference fit. This manufacturing process allowed a thin 2-mm cavity wall of uniform thickness to be manufactured to a high tolerance while reducing the cost. The external surfaces of the cavity are hard anodized to minimize corrosion in the water bath.

Importantly, the cavity water bath mounting arrangement ensures that the entire radiance cavity and the mounting flange remain in contact with water in the bath. The mounting flange is clamped to the inside of the water bath wall using eight M6 bolts, and an insulating washer is used to isolate the mounting flange from the bath wall. This minimizes any thermal gradients occurring at the cavity aperture—a notable problem in the CASOTS-I design.

A high-emissivity paint is required for the internal cavity walls that provides a constant emissivity for the whole cavity, maximizes the radiant energy emitted at the cavity aperture, and minimizes reflection of external source stray radiation effects (Robinson et al. 2010). There are two approaches to managing the internal surface of a thermal infrared blackbody cavity: one can either choose a specular surface (e.g., Geist and Fowler 1986; Fowler 1995) or a diffuse surface (e.g., Mason et al. 1996). Although specular paint surfaces are easier to model using Monte Carlo methods, diffuse paint gives a slightly higher emissivity.

The CASOTS-II cavity is painted using a two-part NEXTEL suede coating 3103 that provides a highly diffusive surface finish with high emissivity in the thermal

infrared region of the electromagnetic spectrum. We measured the hemispherical emittance of NEXTEL suede 3103 for temperatures 273.15–313.15 K using a Bruker VERTEX 70-V Fourier transformed infrared (FTIR) spectrophotometer. Measurements were made using a witness sample coated in exactly the same manner as the CASOTS-II cavity. The hemispherical emittance of NEXTEL suede 3103 is 0.98 ± 0.03, and it shows no temperature variability between 273.15 and 313.15 K (Bras 2013).

The thickness of paint must be as small as possible and homogenous: if the paint is applied as a layer that is too thin, then the surface emissivity characteristics of the CASOTS-II cavity may be influenced by the cavity aluminum substrate; if it is applied as a thick layer, then a temperature difference and time lag may occur between the water bath temperature and the surface of the cavity paint—the latter defining the radiant emission from the cavity (see section 4d for further discussion on this aspect). For the CASOTS-II cavity, the paint is applied uniformly via a spray process following the manufacturer's instructions. The three-part cavity construction of the CASOTS-II blackbody cavity facilitates homogeneity of the painting process because all parts of the cavity can be painted with easy access to internal surfaces before final assembly. Special care is taken to paint the internal surface of the cone section to preserve a sharp internal angle at the cone apex.

A set of interchangeable aperture stop plates that can be mounted on four 4-mm-diameter studs are provided to reduce the cavity aperture to match the field of view of the particular radiometer being tested. The surface of each aperture stop plate is also painted using the same NEXTEL suede 3103 paint used to coat the cavity. An aperture stop plate reduces external stray radiation from entering the blackbody (because the aperture is smaller), but it also increases internal reflections within the cavity, resulting in an increased cavity effective emissivity (by definition, a vanishingly small aperture has an emissivity that approaches 1.0). Finally, an easily removable cover plate is provided to protect the inner surfaces of the blackbody at all times when it is not in use. This reduces ingress of dust and prevents any careless splashing of liquids into the cavity that could reduce the emissivity of the inner surfaces.

c. *Theoretical evaluation of CASOTS-II cavity emissivity*

The CASOTS-II blackbody is modeled first by a computer-aided design (CAD) implementation of its cavity geometry, including front aperture, tubular main body, and cone. We apply a low total (hemispherical) reflectance composed of a dominant ~2.5% diffuse surface scattering contribution (assumed Lambertian in distribution) and a low residual specular contribution (0.1%), in agreement with known ambient-measured properties of such coatings in the 9.5–11.5-μm spectral band. Simulations of the radiance field are then performed via a Monte Carlo ray tracing approach for an isothermal cavity with the aperture fully open (diameter of 110 mm). Cavity effective emissivity values were also derived using simulations with each aperture stop plate installed, varying from 20 to 90 mm in diameter. The ray set is initially constrained to follow the view geometry defined for the ISAR radiometer, that is, diverging from a focus 80 mm in front of the aperture plate and leading to a ~10-mm-diameter beam footprint in its entrance plane. Results are displayed in Fig. 3. Table 1 presents the calculated effective emissivity values for each CASOTS-II aperture stop plate, marked as a dot in Fig. 3. The estimated uncertainty in the results is computed from the ray tracing statistics and is independent of the cavity aperture.

The monotonic dependence of the cavity effective ε on the aperture diameter d can be represented in an empirical model that provides a simple relation linking the cavity theoretical ε with a specific aperture stop plate, written as

$$\varepsilon(d) = 1 - \delta(d), \tag{1a}$$

where δ represents the departure from the perfect blackbody case.

A generic second-order polynomial can be used, with boundary condition $\varepsilon(d = 0) = 1$:

$$\delta_1 = a_1 d^2 + b_1 d. \tag{1b}$$

Expressing d in centimeters, the least squares fit with a 95% confidence interval leads to coefficient values of $a_1 = (6.97 \pm 0.18) \times 10^{-6}\,\mathrm{cm}^{-2}$ and $b_1 = (4.64 \pm 2.25) \times 10^{-6}\,\mathrm{cm}^{-1}$.

Alternatively, the form can represent a direct dependence on an "effective" aperture surface area:

$$\delta_2 = a_2 (d - b_2)^2, \tag{1c}$$

in which case $a_2 = (7.11 \pm 0.10) \times 10^{-6}\,\mathrm{cm}^{-2}$ and $b_2 = 0.18 \pm 0.06$ cm.

For a given cavity geometry, the derived fit coefficients would be ultimately dependent on the inner wall surface properties, dominated here by the residual diffuse reflectance of the NEXTEL paint coating.

The high values of emissivity predicted by this approach prompted some further investigation of the sensitivity to the model assumptions concerning the surface

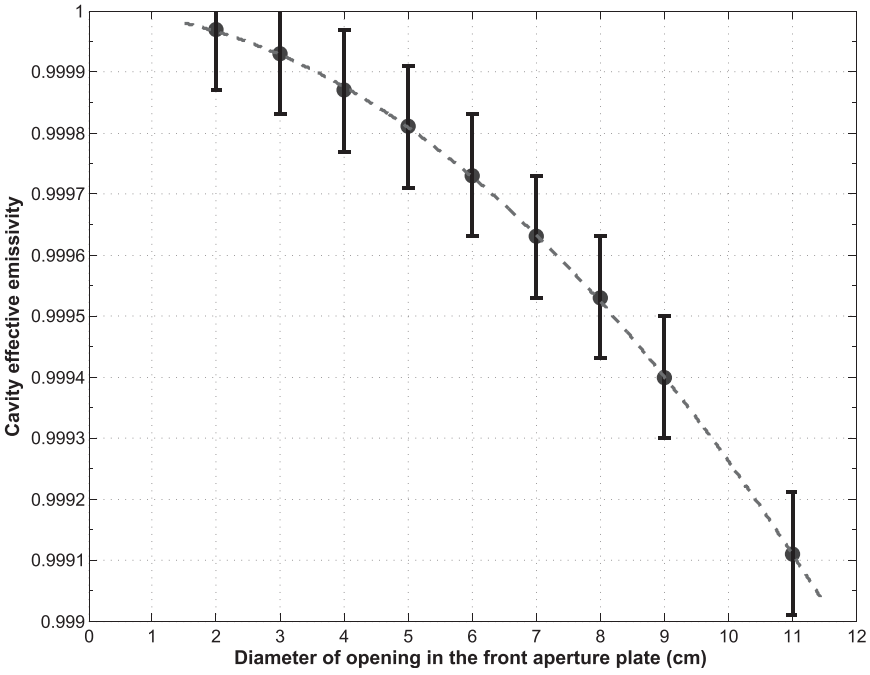

FIG. 3. Results from Monte Carlo simulation estimates of the CASOTS-II cavity effective ε as a function of aperture diameter d for a fully open cavity of 110-mm diameter and with each front aperture plate of different diameters installed. The dashed curve is an empirical model based on the fit to the computed values.

emissivity within the cavity. A fixed front aperture plate with a 90-mm-diameter opening is used for comparison. The results of the simulations indicate that even a hundredfold increase of cavity inner surface specular reflectance (from 0.1% to 10%) still leads to $\varepsilon > 0.9975$, indicating the excellent geometrical trapping behavior of the cavity design. If the inner wall diffuse reflectance is now varied to values higher than 10%, then a significant decrease in cavity effective emissivity is found dropping to $\varepsilon < 0.985$ when the diffuse reflectance is set arbitrarily to 25%.

The assumption of Lambertian behavior for the surface scattering radiative exchanges may not be fully valid. Other black coatings with similar dominant residual diffuse reflectance have displayed, based on ambient measurement at $\sim 10\,\mu$m (see Persky 1999; and associated references), a nonconstant surface bidirectional reflectance distribution function (BRDF) with a noticeable increase in near-specular directions at high incidence and scattering angles. Maintaining a total integrated scatter limit of 2.5%, such a BRDF was applied to the 90-mm aperture stop case that indicated a reduction of ε from 0.9994 to 0.9905. In absolute terms such an impact on ε is acceptable, but it indicates that a small and realistic departure from Lambertian surface BRDF can also affect the cavity performance as a whole.

For a given isothermal cavity geometry, any spectral dependence of the effective emissivity would be dominated by the spectral variations of the cavity paint. The NEXTEL black coating 3103 exhibits quasi-flat variations between ~2.0% and ~2.5% at ambient temperature for its dominant diffuse reflectance over the ~3- to ~30-μm spectral range. Secondary effects, such as wavelength-dependent aperture diffraction, have indicated small corrective variations to ε across a ~20% spectral bandwidth centered around 10.5 μm. The linear wavelength dependence over this band leads to a limited degradation of the nominal cavity effective emissivity

TABLE 1. Theoretical ε values for each CASOTS-II aperture stop plate indicated as a dot in Fig. 3.

Aperture diameter (mm)	Effective ε (± 0.0001)
20	0.999 97
30	0.999 93
40	0.999 87
50	0.999 81
60	0.999 73
70	0.999 63
80	0.999 53
90	0.999 40
110	0.999 11

to ~0.9988 at 11.5 μm and ~0.9990 at 9.5 μm for the smallest aperture case of 20-mm diameter. This is still about 2000 times the central wavelength and does not generate a strong diffractive spread. The slight reduction of spectral diffuse reflectance for the NEXTEL black coating from 9.5 to 11.5 μm will compensate for this effect, so that in the end the spectral cavity emissivity will be constant and therefore its band-integrated average value will not differ from the nominal results. Ultimately, it will depend on the in-band and out-of-band responses of the sensor viewing the blackbody, but this situation would no longer represent an intrinsic characteristic of the CASOTS-II performance.

We calculate an uncertainty for the CASOTS-II surface paint in the following manner. For a high-emissivity blackbody with a diffuse surface coating, the figure of merit

$$f = (1 - \varepsilon_{\text{coating}})/(1 - \varepsilon_{\text{BB}}) \tag{2}$$

is almost constant for small variations in the coating emissivity $\varepsilon_{\text{coating}}$ and is determined by the geometry of the blackbody cavity. Consequently, we can estimate the change in the blackbody emissivity $\Delta\varepsilon_{\text{BB}}$ for a change in coating emissivity $\Delta\varepsilon_{\text{coating}}$ using

$$\Delta\varepsilon_{\text{BB}} = \Delta\varepsilon_{\text{coating}}/f \tag{3}$$

and the corresponding changes in blackbody radiance ΔL_{BB} and brightness temperature ΔT_{BB} using

$$\Delta L_{\text{BB}} = \Delta\varepsilon_{\text{BB}}[B(\lambda, T_{\text{BB}}) - B(\lambda, T_{\text{ambient}})] \quad \text{and} \tag{4}$$

$$\Delta T_{\text{BB}} = \Delta L_{\text{BB}} \Big/ \left.\frac{\partial B}{\partial T}\right|_{\lambda, T_{\text{BB}}}, \tag{5}$$

respectively, where $B(\lambda, T)$ is the Planck function and T_{BB} and T_{ambient} are the blackbody cavity and ambient temperatures. We calculate an uncertainty for the CASOTS-II surface coating in the following way. For the worst case of a 110-mm aperture, the figure of merit is approximately 28. Observing at 10.5 μm in an ambient temperature of 293.15 K and for a worst-case decrease of 0.03 in a coating emissivity of 0.98, the brightness temperature of the cavity would fall by 43 mK at 340 K and rise by 28 mK at 270 K. For a 40-mm aperture, the figure of merit is approximately 326 and these changes are reduced to just 6.2 and 4.1 mK, respectively. We use these worst-case estimates of calculated temperature uncertainty due to the surface coating in the uncertainty budget for the CASOTS-II cavity (see section 4f).

d. *Effect of stray radiance*

As the CASOTS-II cavity does not have an emissivity value of 1.0, adjustment must be made to compensate for reflected "stray" radiance. Potentially, stray radiance will originate from many areas within the laboratory in front of the CASOTS-II aperture. In practice, strays are largely limited to the front face of the ISAR radiometer when installed on its cradle viewing the CASOTS-II cavity. We computed the radiometric temperature error for a radiometer viewing the CASOTS-II cavity at a wavelength of 10.5 μm for a worst-case emissivity of 0.9991 (full aperture) and best-case emissivity of 0.9999 (the typical 40-mm aperture plate in place for an ISAR radiometer) for a range of typical CASOTS-II water bath temperatures. For these calculations we assumed a constant room temperature (T_{room}) of 293.15 K. The results of these calculations are shown in Fig. 4 and they reveal worst-case ($\varepsilon = 0.9991$, $T_{\text{room}} = 293.15$ K) errors of +23 mK ($T_{\text{casots}} = 270$ K) and −36 mK ($T_{\text{casots}} = 340$ K). The best-case ($\varepsilon = 0.9999$, $T_{\text{room}} = 293.15$ K) errors are +3 mK ($T_{\text{casots}} = 270$ K) and −4 mK ($T_{\text{casots}} = 340$ K), highlighting the importance of installing the smallest aperture stop plate possible for each viewing radiometer configuration.

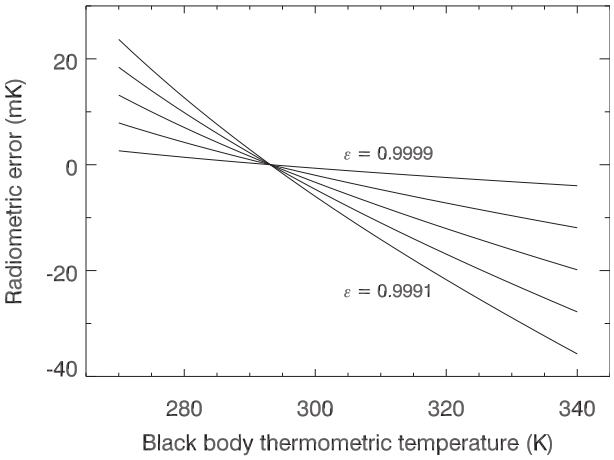

FIG. 4. Radiometric temperature error of the CASOTS-II cavity due to stray radiance for a radiometer viewing the CASOTS-II cavity at a wavelength of 10.5 μm for a "worst case" emissivity of 0.9991 (full aperture) and "best case" emissivity of 0.9999 (40-mm aperture plate in place) over the operating range of CASOTS-II water bath temperatures. For these calculations, we assumed a constant room temperature of 293.15 K.

The errors shown in Fig. 4 are known errors rather than systematic uncertainties in bias. These can in principle be calculated based on adequate knowledge of the radiative temperature of the stray radiance (e.g., ambient room temperature or the temperature of the front face of the radiometer viewing the CASOTS-II cavity if close enough). A suitable uncertainty estimate could then be derived from the uncertainties in the CASOTS-II emissivity and background radiance depending on the individual instrument setup and laboratory

TABLE 2. Standard uncertainty budget for the CASOTS-II water bath thermometry system.

Item	Standard uncertainty (K)
Thermometrics ES225	0.0015
Steinhart–Hart equation	0.003
Stability K yr^{-1}	0.005
Hart Scientific 1504 bridge	0.003
Overall RSS uncertainty	0.0067

environment. This is in fact the method used during ISAR calibration validation experiments.

4. Performance of the CASOTS-II

a. Water bath temperature measurement system

The CASOTS-II water bath temperature is measured using a Hart Scientific 1504 temperature bridge accurate to ±0.003 K at 298 K and a Themometrics ES 225 temperature probe. The temperature probe is mounted through a hole in the water bath lid with the sensing tip located ~10 mm away from the cavity cone surface. The CASOTS-II reference blackbody achieves SI traceability via the thermometer system used to measure the water bath temperature. The Hart thermometer system used here is regularly calibrated completely against a standard thermometer, traceable to the U.K. National Physical Laboratory realization of the International Temperature Scale of 1990 (ITS-90). Table 2 provides an uncertainty budget for the CASOTS-II water bath thermometry system that has a standard uncertainty of 0.0067 K.

b. Cavity aperture temperature gradients

During a calibration experiment at the University of Miami Rosenstiel School of Marine and Atmospheric Science (RSMAS), a thermal camera (ThermaCAM SC3000 NTS, SN-1210014, NOF Filter and Lens 20) was used to obtain thermal imagery of the CASOTS-II cavity at a variety of operating temperatures. The ThermaCAM operates in the 8–9-μm wave band and has an accuracy of ±1% or ±1 K and precision of 0.02 at 303 K, although the relative accuracy of the camera was found to be superior. The top panel in Figure 5 displays a processed example from this dataset showing the CASOTS-II cavity to have a mean flat response across the aperture (within the apparent 0.1-K accuracy of the ThemaCAM measurement) at a temperature of ~290 K. The bottom panel in Fig. 5 plots data extracted along the transect lines across the CASOTS-II cavity aperture diameter shown in the top panel superimposed onto a single plot. The panels in Figs. 6 show similar plots obtained when the CASOTS-II cavity was operated at a temperature of ~310.5 K.

There is a systematic increase in thermal camera charge-coupled device (CCD) noise to the left of the top panels in Figs. 5 and 6 that persisted for all measurements taken by this particular ThermaCAM 3000 camera. It is thought to relate to the camera CCD calibration, as this feature was also present when viewing other blackbody cavities. Allowing for this, Figs. 5 and 6 show no evidence of thermal gradients at the lip of the CASOTS-II blackbody aperture. In addition to this analysis, ThermaCAM 3000 animations of the CASOTS-II aperture obtained over several minutes and at different cavity temperatures confirm that the water bath does not introduce any persistent temperature gradients across the CASOTS-II cavity measurable at the precision of the ThermaCAM system.

c. Temperature drift of the CASOTS-II water bath

Although the proprietary tank used as the CASOTS-II water bath has the capacity for cooling and heating the bath, these features are not used and there is no direct temperature control of the water bath. Water bath systems are available with mK stability e.g., Geist and Fowler 1986) but they are expensive. For the primary purpose of independently verifying the calibration of ISAR seagoing infrared radiometers, the CASOTS-II water bath is heated slowly by the immersed water bath pump unit. A typical ISAR radiometer calibration run at an ambient room temperature of ~293 K begins by filling the water bath with water at ~288 K which, after continuously stirring by the pump with the water bath lid closed, increases to ~312 K over a ~15-h period. The thermal input of the pump gradually approaches equilibrium with heat loss via the cavity aperture and water bath walls, so that the water bath temperature stabilizes unless further heating or cooling is provided. This dynamic approach to calibration is suitable only for radiometers such as ISAR that have relatively fast (~10 s or less) measurement sample times. We note that when calibrating radiometers that require several minutes to complete a measurement cycle (e.g., M-AERI; see Minnett et al. 2001), an accurate and stable set-point reference blackbody source is preferable (e.g., Fowler 1995, 1996).

Based on 9 years' experience working with the ISAR radiometer and the CASOTS-II blackbody, we have found that this drifting water bath temperature design satisfies our requirement to calibrate the ISAR radiometers to better than ±0.1 K. To ensure that this criterion is met, the water bath temperature evolution error on the calibration must be $\ll$0.1K. In the case of the ISAR radiometer, measurements are acquired at 1-s intervals (during ship operations these are further averaged to ~30-s intervals). If temperature changes

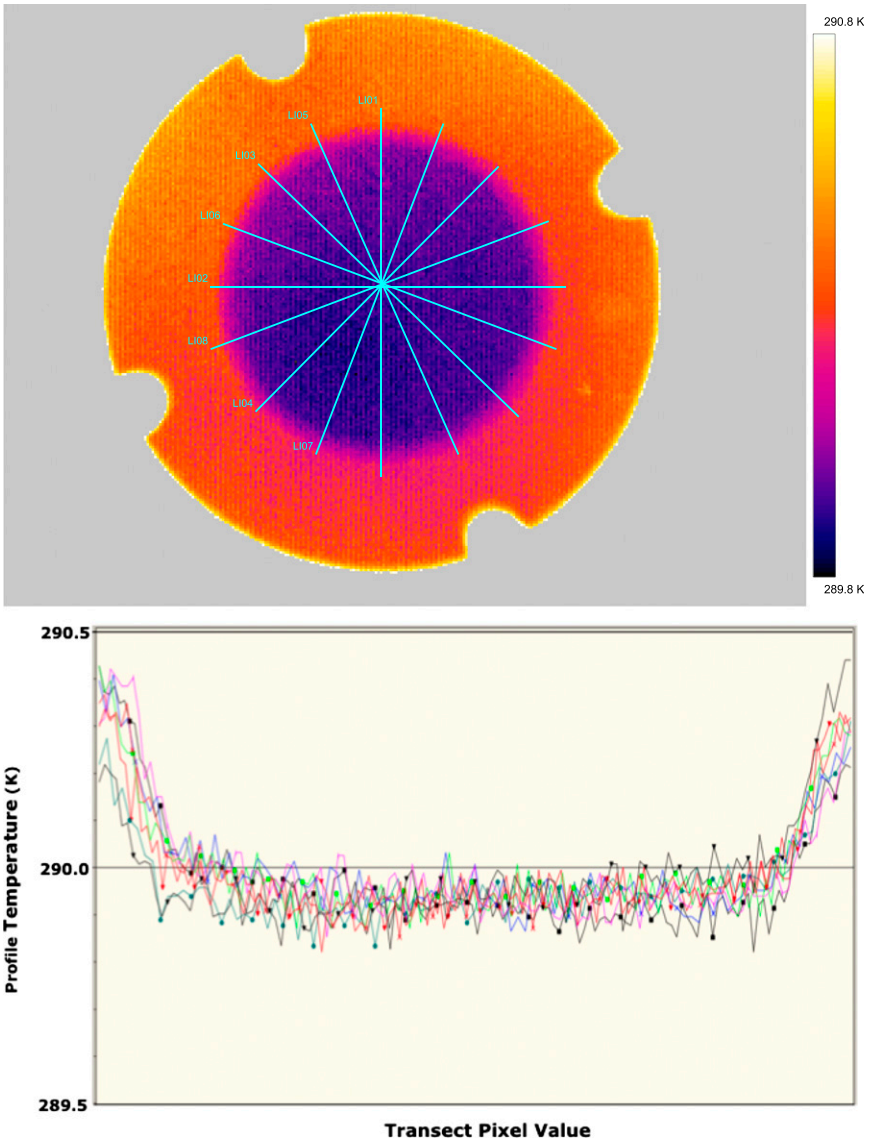

FIG. 5. (top) FLIR ThermaCAM SC3000 NTS image of the CASOTS-II blackbody full aperture for a cavity temperature of 289.9 K. The ambient room temperature at the time of image acquisition was ~289 K. The pale blue lines correspond to the position of the profiles displayed with dots in the (bottom) panel; the colors of the non-dotted profiles are for different sampled diameters.

during an individual sample are not to introduce additional errors, we can set a worst-case upper bound on the water bath heating rate equivalent to half the measurement uncertainty (Table 2) per sample interval. Thus, the heating rate of the water bath must be $<0.0067\,(2\,\mathrm{K\,s^{-1}})^{-1}$, that is, $0.20\,\mathrm{K\,min^{-1}}$ or $12\,\mathrm{K\,h^{-1}}$. This is the limit of what was possible using the previous CASOTS-1 design.

Figure 7a presents the CASOTS-II water bath heating rate, in kelvins per hour, evaluated from the heating profiles recorded during more than 100 ISAR calibration runs across a CASOTS-II temperature range of 275–320 K, performed during 2004–12. The number of data points used to construct Fig. 7a are shown in Fig. 7c. Each calibration run took ~(15–20) h to complete. Data shown for CASOTS-II temperatures below 286 K were obtained in a temperature-controlled cool room maintained at 278 ± 2 K. Such calibration runs are only performed a few times per year during the winter season to check the calibration of ISAR radiometers in cooler ambient temperatures and/or to avoid condensation effects on the CASOTS-II cavity at lower temperatures. The sample number of calibrations for the cool-room

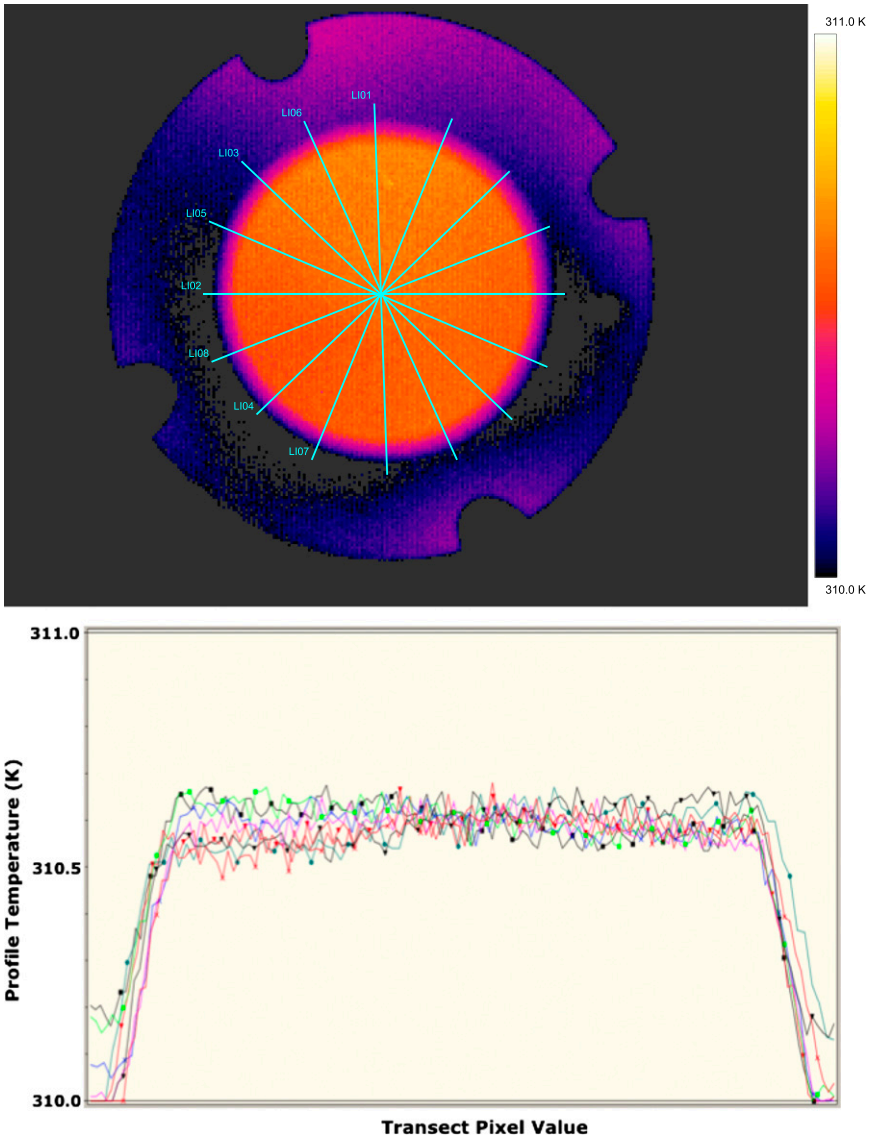

FIG. 6. As in Fig. 5, but for a cavity temperature of ~310.5 K.

cases is therefore small (Fig. 7c). Data shown for temperatures above 286 K were obtained in uncontrolled ambient laboratory temperatures between 291 and 300 K with a median of 293 K. The fitted line is a least squares linear fit to the data that has been binned into 1-K temperature bins. Other bin sizes have been tested but do not change the result. The dot indicates the mean value of all calibration data at that temperature bin for all calibration runs. Uncertainty estimates in Fig. 7a are computed as the standard deviation from the mean of all calibration data obtained at that temperature bin.

The data show that the modal mean heating rate of the CASOTS-II blackbody water bath using the Hozelock Cascade 4000 LV pump is 0.6 K h^{-1} (0.01 K min^{-1}), which is significantly less than the CASOTS-I design. As expected, higher heating rates of up to 1.4 K h^{-1} (0.023 K min^{-1}) are apparent at the extreme lower water bath temperatures but remain well within the required limit of 0.20 K min^{-1}. At progressively higher water bath temperatures, the heating reduces to negligible rates as thermal balance is reached between heat input from the water pump and heat loss from the water bath walls and through the blackbody cavity aperture.

For the purpose of estimating the uncertainty arising from the CASOTS-II temperature drift, we consider the worst-case heating rate of 0.023 K min^{-1}, computed using a 20-s integration time for the radiometer being tested, which is 20 times longer than that normally used when validating an ISAR. If no allowance is made for the rise in the CASOTS blackbody temperature during

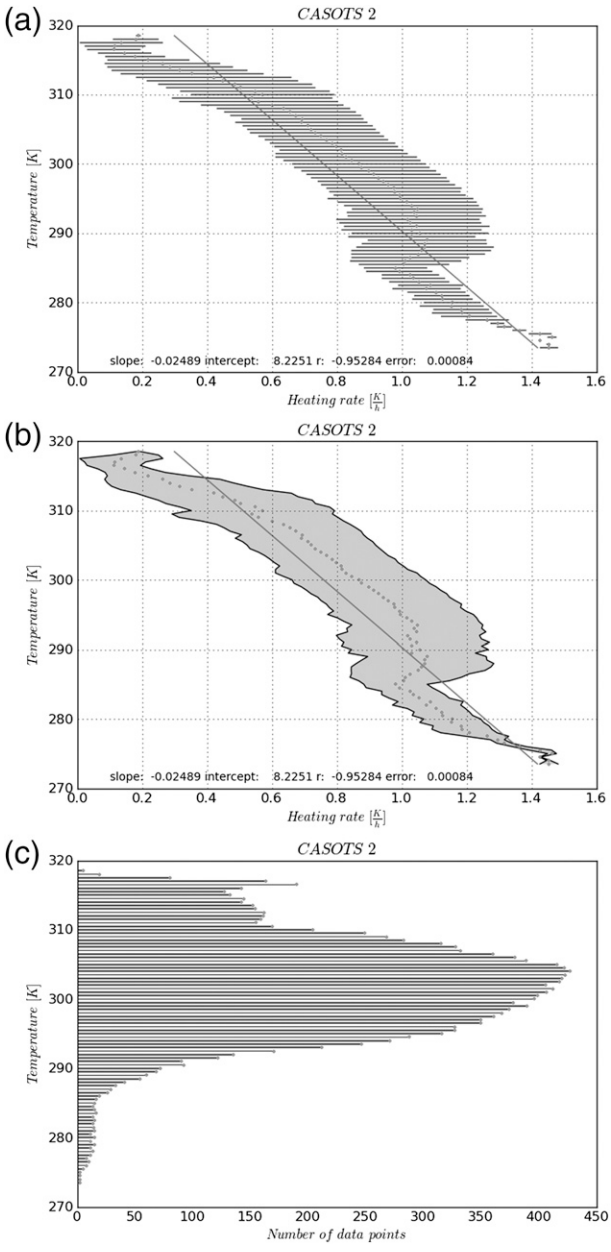

FIG. 7. (a),(b) Dependence of CASOTS-II water bath heating rate on the water bath temperature computed from a large range of calibration runs over a temperature range of 275–320 K. Data for temperatures < 286 K were obtained in controlled cool rooms maintained at 278 ± 2 K and >286 K in uncontrolled ambient laboratory conditions. The fitted line is a least squares linear fit to the data in 1-K bins. The horizontal lines in (a) and the gray area in (b) are the uncertainty estimates computed as the standard deviation from the mean of all calibration data obtained within a given temperature bin (dots). (c) Number of data points used to compute the CASOTS-II heating rates.

the integration time, then the resulting uncertainty is 0.0076 K.

The worst-case phase measurement error between ISAR radiometer measurements and the CASOTS-II cavity temperature (assuming a worst-case error of 2 s, i.e., ±1-s clock error in either the Hart or the ISAR clocks) is <0.0008 K, which is negligible for our stated application.

d. Thermal gradients within the water bath

Although the submersed pump is slowly heating the water bath, it is important to verify that the water bath is well mixed and that temperature gradients in the bath are not present at the level of accuracy required for ISAR calibrations. Extensive investigations of the water bath uniformity have been performed by comparing our Hart Scientific water bath temperature measurements made at the reference measurement position and simultaneous water bath temperature measurements obtained using an SBE 38 thermometer (Sea-Bird Electronics, Inc. 2011). The SBE 38 sensor had an accuracy of ±0.001 K and a resolution of 0.25 mK over the water bath temperature range. We made measurements at a nominal water bath temperature of 289 K and 309 K, and ambient temperature of 294.5 K. Measurements were made using the SBE 38 at four corner positions of the CASOTS-II water bath close to the cavity walls toward the bottom of the bath. Each time the SBE 38 probe was moved to a new position, no measurements were recorded until the water bath circulation was reestablished (typically ~30 s due to the large volume capacity of the running water pump). We allowed at least 60 s before recording any new measurements at different probe positions. We measured at four physically distinct and extreme locations in the water bath relative to the Hart thermistor sequentially several times at two nominal temperatures. We then computed the mean difference between the Hart-measured water bath temperature and the temperature measured by the SBE at each position. The results are presented in Table 3.

The water bath lid could not be fully closed due to the SBE 38 cable exit, which may explain the larger temperature differences at the hot water bath temperatures, although these differences are close to the combined uncertainty of the Hart and SBE 38 measurement system. The worst-case temperature nonuniformity values show that the bath is well mixed to 0.0096 K.

e. Temperature drop across the cavity wall and paint

The actual temperature of the CASOTS-II internal surface coated with NEXTEL 3103 paint can be slightly different from the value of the water bath measured by the temperature sensor. The thin layer of paint acts as an insulator (with a specific thermal conductivity and finite heat capacity), and its temperature may lag in time compared to the cavity wall temperature beneath it (although these effects only become important if the paint thickness

TABLE 3. CASOTS-II water bath temperature difference between the Hart reference thermometer and the SBE 38 temperature sensor at the four corner positions in the water bath. Run 1 was obtained at a water bath temperature of 289 K and run 2 at 309 K. Ambient temperature was 294.5 K.

Position	Temp (K)	Hart − SBE 38 (K)
1	289	0.0013
2	289	0.0012
3	289	−0.0009
4	289	0.0030
Overall RSS uncertainty		0.0036
1	309	−0.0040
2	309	0.0029
3	309	−0.0051
4	309	−0.0065
Overall RSS uncertainty		0.0096

is significant (e.g., Robinson et al. 2010). The black paint must be applied as a thin layer to minimize 1) the temperature difference between the water bath temperature and the internal painted surface of the cavity (related to paint thickness and the geometric configuration of the cavity) and 2) the thermal drag-down effect (McKelvie 1987). Thermal drag down is related to both the impedance of the cavity wall (paint and aluminum wall) and the variability of the thermal load: if the variability is too high, then heat will not flow through the cavity wall and its paint fast enough to maintain a temperature identical to the water bath. In the case of the CASOTS-II design, thermal load variability can be neglected because it is extremely low.

Worst-case approximations are used to estimate the temperature difference across the CASOTS-II cavity. We derive a generic configuration or view factor dF for the effective global radiative exchange between the entire CASOTS-II cavity (in practice dominated by the directly viewed cone region) and the cavity aperture. Following the approach of Fowler (1995),

$$1 - \varepsilon = (\rho_{ss}\rho_{sh})^2 + \mathrm{dF} \times \rho_d, \tag{6}$$

where ρ_{sh} is the specular reflectance of the cavity surface at high angles of incidence (AoI), ρ_{ss} is the specular reflectance of the cavity surface at smaller AoI, ρ_d is the in-band diffuse reflectance of NEXTEL black paint (~2.5%), and ε is derived from Monte Carlo model simulations. The $1 - \varepsilon$ term for CASOTS-II is equivalent to the residual function $\delta(d)$ [Eq. (1)] parameterized for the set of d. For the CASOTS-II internal coating, the in-band specular reflectance is very low (~0.1%) and the first quadratic term in the above-given expression is completely negligible. We can then write

$$\mathrm{dF} \approx \frac{1 - \varepsilon}{\rho_d} = \delta(d)/\rho_d. \tag{7}$$

The general configuration factor dF for the CASOTS-II cavity relates the exchange between (or through) surfaces and varies as d^2. Because the CASOTS-II cavity is considered isothermal at a given instant and dF is derived from the computed cavity-level emissivity, it is applicable for all internal geometrical view factor effects as well as the reflection and scattering process for radiative transfer calculations.

Considering the temperature difference across the wall of the cavity, following Fowler [1995, Eq. (2)] we can write

$$\mathrm{dP} = \frac{(T_o - T_{\mathrm{int}})}{\left(\frac{d_{\mathrm{wall}}}{K_{\mathrm{wall}}} + \frac{d_{\mathrm{nx}}}{K_{\mathrm{nx}}}\right)}, \tag{8}$$

where dP is differential heat conduction across the cavity wall and radiating out of the cavity; T_o is the water bath temperature and T_{int} is the temperature of the blackbody cavity paint surface (i.e., the radiating surface within the blackbody viewed by an external radiometer); d_{wall} and K_{wall} are the thickness and thermal conductivity of the aluminum cavity wall, respectively; and d_{nx} and K_{nx} are the thickness and thermal conductivity of the NEXTEL suede 3103 paint, respectively. We assume that the surface of the cavity in contact with the water bath is at a uniform water bath temperature T_o. The thickness of the aluminum cavity wall is uniformly 2 mm. The thickness of the NEXTEL suede 3103 paint has been measured using the difference between the thickness of painted and nonpainted witness samples, and was found to be 0.055 mm. We note that a typical spray coating has a thickness variation of the order 5 μm, although we do not expect this to influence our results for the temperature regimes in which the CASOTS-II blackbody operates. Obtaining information on the thermal conductivity of thin paint layers is challenging (e.g., Legaie et al. 2008) and we assume a worst-case approximation for the thermal conductivity of NEXTEL suede 3103 paint of 0.0009 W $(\mathrm{cm\,K})^{-1}$ based on the value published by Fowler (1995).

Considering the net effective exchange between the whole painted cavity wall and the ambient external environment viewed through the cavity aperture,

$$\mathrm{dP} = \mathrm{dF} \times \sigma(T_{\mathrm{int}}^4 - T_o^4), \tag{9}$$

where σ is the Stefan–Boltzmann constant, and applying a temperature difference approximation using

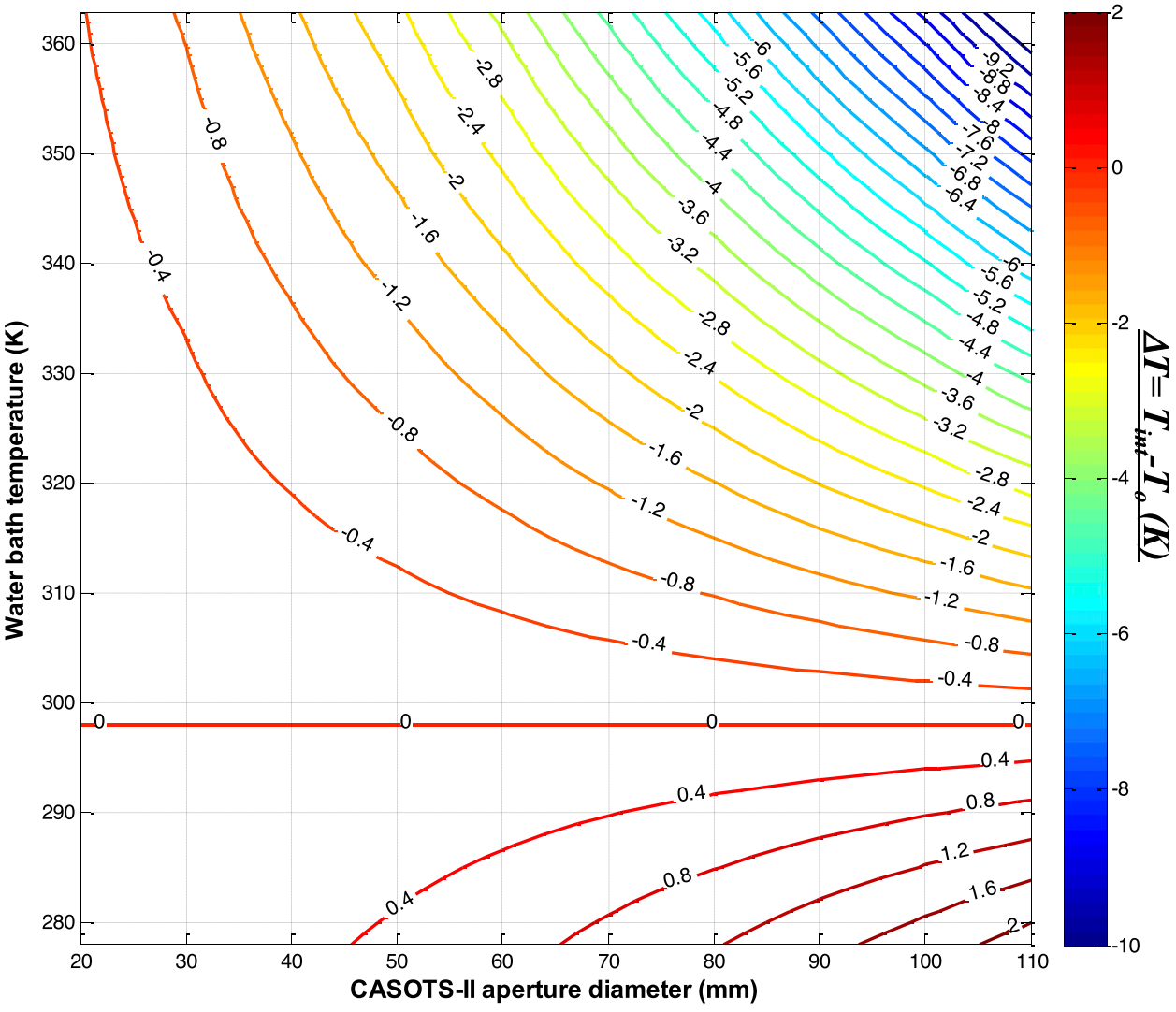

FIG. 8. Calculations of the temperature difference, $\Delta T = T_{\text{int}} - T_o$, across the CASOTS-II cavity wall and NEXTEL suede 3103 paint for different water bath temperatures T_o and internal NEXTEL paint surface T_{int} for ambient room temperature of 298 K as a function of CASOTS-II viewing aperture diameter.

$$T_{\text{int}}^4 \approx T_o^4 + 4T_o^4 \Delta T, \tag{10}$$

we can calculate the temperature difference across the CASOTS-II cavity wall, $\Delta T = T_{\text{int}} - T_o$, expressed as

$$\Delta T = \frac{-\beta(T_{\text{int}}^4 - T_{\text{ext}}^4)}{1 + 4\beta T_o^3} \tag{11a}$$

with

$$\beta = K \times \text{dF} \times \sigma, \tag{11b}$$

where K is equal to the denominator term in Eq. (8) and T_{ext} is the assumed temperature of the external environment.

Figure 8 presents ΔT calculated for an ambient external temperature T_{ext} of 298 K as a function of water bath temperature and cavity aperture diameter; ΔT has a range from -2 to $+10$ mK in the worst-case condition using a full 110-mm aperture. For an ISAR radiometer viewing the CASOTS-II cavity with an aperture stop plate of 40-mm diameter, ΔT has a value of <1.6 mK for all water bath temperatures. We note that rarely, if ever, is the CASOTS-II water bath temperature above 340 K when validating radiometers for use in satellite SST validation experiments, placing a realistic upper limit of 6 mK on the value of ΔT for full aperture and 1 mK for a 40-mm aperture.

TABLE 4. Overall worst-case uncertainty estimate for the CASOTS-II blackbody cavity for the full aperture case and with the 40-mm aperture stop plate in place.

Source of uncertainty	Standard uncertainty for full aperture (K)	Standard uncertainty 40 mm aperture (K)
Uncertainty in NEXTEL paint emissivity (section 3c)	0.043	0.0062
Stray radiance error (see section 3d and Fig. 4: $T_{room} = 293.15$ K and $T_{casots} = 340$ K)	0.036 ($\varepsilon = 0.9991$)	0.004 ($\varepsilon = 0.9999$)
Thermometry system (section 4a; Table 2)	0.0067	0.0067
Heating rate error (section 4c)	0.0076	0.0076
Worst-case water bath thermal gradients at 309 K (section 4d; Table 3)	0.0096	0.0096
Cavity wall–paint thermal gradient (taken from Fig. 8 for a worst-case water bath temperature of 340 K; section 4e)	0.006	0.001
Overall RSS uncertainty (K)	0.058	0.016

f. Overall standard uncertainty budget for the CASOTS-II blackbody system

The total standard uncertainty of the water bath temperature measurement may be calculated as root-sum-square (RSS) standard uncertainties resulting from the Hart thermometer electronics (Table 2), heating rate error, water bath nonuniformity, uncertainty of the paint emissivity, thermal gradients across the painted cavity wall, and stray radiance. The results are shown in Table 4, based on worst-case scenarios discussed in detail in the foregoing sections. The standard uncertainty for the CASOTS-II blackbody with a 40-mm aperture is 16 mK, which is more than adequate for calibrating ISAR radiometers for use in satellite SST validation activities. In this case, the larger sources of uncertainty come from the possibility of thermal gradients in the water bath, the gradual rise of the water bath temperature, and the accuracy and stability of the thermometry.

When used with the 110-mm aperture, the standard uncertainty rises to 58 mK. The increase results from radiative uncertainties associated with the paint emissivity and stray radiation terms that grow to dominate the uncertainty budget.

g. SI traceability of the CASOTS-II blackbody

The procedure of pre- and postdeployment calibration of shipborne radiometers using the CASOTS-II blackbody makes it possible, in principle, to apply rigorous quality control that satisfies the requirements of the Group on Earth Observations (GEO) and CEOS Quality Assurance Framework for Earth Observation (QA4EO) (QA4EO Task Team 2010) approach to delivering climate quality data. However, this can only be achieved in practice if the accuracy of the CASOTS-II system is traceable to an international standard. With this objective, the CASOTS-II was entered into a CEOS Working Group on Calibration and Validation (WGCV) Infrared Visible Optical Sensors (IVOS) subgroup radiometer intercomparison experiment performed at the U.K. National Physical Laboratory (NPL) and at RSMAS in 2009. The objectives of the 2009 comparison were to establish the "degree of equivalence" between terrestrially based infrared validation measurements made in support of satellite observations of the earth's surface temperature and to establish their traceability to the SI through the participation of national metrology institutes (Theocharous and Fox 2010; Theocharous et al. 2010). As part of this activity, several blackbodies were compared to reference standards using NPL's reference transfer radiometer [Absolute Measurements of Blackbody Emitted Radiance (AMBER; see Theocharous et al. 1998) and the NIST Thermal-Infrared Transfer Radiometer (TXR; e.g., Rice et al. 2004). Comparisons made at RSMAS between water bath temperatures and NIST TXR measurements of the CASOTS-II and the Miami reference calibration blackbodies showed agreement within the combined uncertainties of the TXR instrument (44 mK; Theocharous and Fox 2010) and the two blackbodies measured at Miami (Theocharous and Fox 2010). Table 5 shows the results from comparing the CASOTS-II cavity temperatures determined by the AMBER radiometer and those estimated from the CASOTS water bath thermometer, viewed at three different nominal temperatures (283, 293, and 202 K) repeated on two adjacent days. The largest temperature differences were less than ±20 mK for all three temperatures and are well within the combined uncertainty of the measurements by the AMBER radiometer (48 mK; Theocharous and Fox 2010). These data confirm that the CASOTS-II blackbody can be used as an absolute infrared reference source at 10 μm, traceable to NPL standards. Using our worst-case uncertainty budget in Table 4, the combined

TABLE 5. Results from comparison tests between the CASOTS-II blackbody temperature as measured by the NPL AMBER radiometer and the CAOTS-II water bath temperature as measured by a Hart platinum resistance thermometer.

Nominal temp (K)	Temp diff (AMBER − CASOTS-II water bath), 21 Apr 2009 run (mK)	Temp diff (AMBER − CASOTS-II water bath), 22 Apr 2009 run (mK)
303	−7	3
293	−16	−14
283	−19	−18

uncertainty of the comparison to AMBER is 75 mK [i.e., $(58\,\mathrm{mK}^2 + 48\,\mathrm{mK}^2)^{1/2}$]. When calibrating an ISAR radiometer with a 40-mm aperture in place, this reduces to 50 mK.

5. Application of the CASOTS-II using the ISAR radiometer in the Bay of Biscay

This section illustrates the benefit of using the CASOTS-II blackbody in support of autonomous routine shipborne radiometer deployments.

a. Using the CASOTS-II to quantify absolute uncertainty in ISAR measurements

ISAR deployments aboard a ferry ship operating in the Bay of Biscay have been executed since 2004 to deliver an independent and objective assessment of the accuracy of the SST data retrieved from the *Environmental Satellite* (*Envisat*) Advanced Along-Track Scanning Radiometer (AATSR; Wimmer et al. 2012). ISAR deployments are typically ~3 months and are fully automated. The ferry repeatedly sailed a regular 3-day passage from Portsmouth, United Kingdom, to Bilbao in northern Spain and back, traversing the English Channel and Celtic Sea shelf seas and the deep Atlantic Ocean Bay of Biscay. A deployment ends when an ISAR is removed from the ferry to be serviced and is replaced by another instrument to continue the deployment. To date there have been more than 30 separate deployments of an ISAR, during which the $\mathrm{SST_{skin}}$ measurements are continuously acquired (except during precipitation events) along the ship track at 1-s sampling intervals averaged to 4-min mean values of $\mathrm{SST_{skin}}$. More than 1500 independent measurements from ISAR and *Envisat* AATSR coincident within specified space–time matching windows have been obtained, proving that the systematic use of autonomous underway shipboard radiometry on a vessel of opportunity for validating satellite data is today a reality.

The first infrared blackbody of the CASOTS-II design (serial 001) was built in 2005 and has been used since then to provide regular quality control of the ISAR radiometer. Prior to deployment, an ISAR instrument is inspected, cleaned, damaged or degraded optical components (e.g., the gold scan mirror) are replaced, and the ISAR optical alignment is verified before the instrument is reassembled, ready for its next deployment. ISAR radiometers are not deployed unless a CASOTS-II laboratory validation quantitatively demonstrates that measurements are accurate to within ±0.1 K of the brightness temperature of the CASOTS-II cavity. The CASOTS-II predeployment validation is essential because it establishes the absolute accuracy of each instrument with SI traceability of the measurements as well as identifies any instrument problems prior to deployment.

Figure 9 shows a typical example calibration before deployment that spans the range 295–313 K over a 23-h period in September 2008. To begin each calibration, ISAR is installed in the cradle in front of the CASOTS-II blackbody and carefully aligned with the cavity aperture as shown in Fig. 10. The water tank is filled and its temperature adjusted (typically using cold water or ice, allowing any ice to fully melt before measurements begin) to set the starting temperature to a few kelvins below the range of temperatures expected during the deployment but above the dewpoint temperature of the laboratory atmosphere. The water bath lid is closed and a short period (~10 min) is allowed for the tank to become well stirred and also to allow time for the air in the CASOTS-II cavity to attain a quasi-steady state with respect to the temperature of the water bath. It should be recognized that the air within the cavity will, relative to the ambient room temperature, be subject to small local convective exchange with the ambient laboratory as the CASOTS-II temperature changes. Such convective flows are expected to be negligible, as the cavity is heated so slowly. Furthermore, we note that the most important CASOTS-II measurements for our application using the ISAR radiometer are made over the fairly limited temperature range encountered at the sea surface and for which the convective flow in laboratory validations is smallest. To minimize this effect, our best-practice approach is to minimize any activity in the laboratory during a calibration run.

Calibrations are run over several hours to simulate sustained operation at sea, and they span the range of temperature differences, positive and negative, between

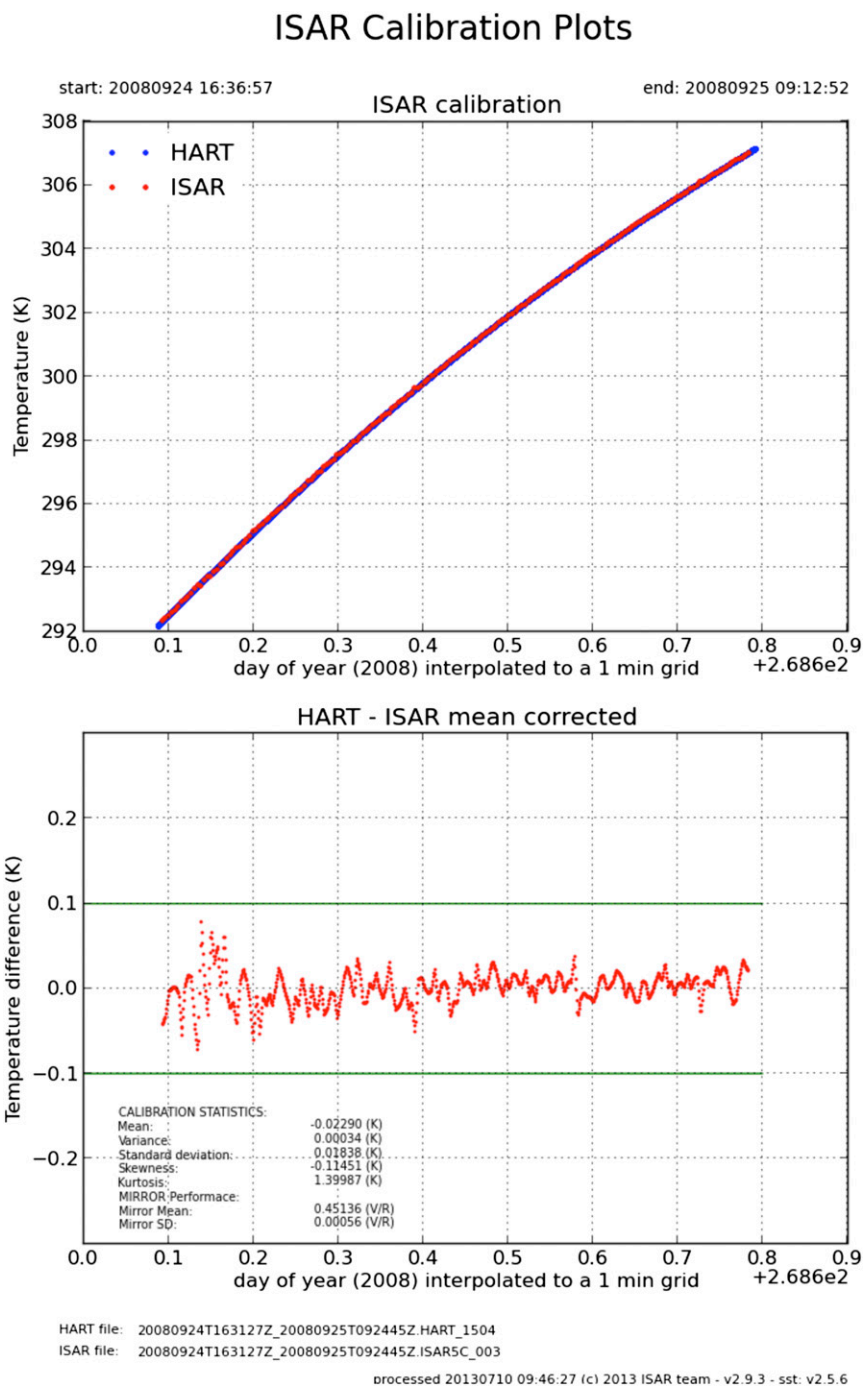

FIG. 9. Predeployment calibration of ISAR-003 prior to operations in the Bay of Biscay, 24 Sep 2008. (top) The CASOTS-II temperature included in the calibration measured by the ISAR and the CASOTS-II thermometry. (bottom) The residual difference between the ISAR-determined CASOTS-II temperature and the measured water bath temperature.

the target and the ambient temperature of the ISAR radiometer. The procedure outlined above achieves a good simulation of the northeast Atlantic SST regime encountered during deployments with differences between ambient and SST_{skin} of about -5 to $+10$ K. To test the ISAR performance in more extreme meteorological conditions in which the ISAR ambient temperature may be significantly different from the SST, ISAR validation

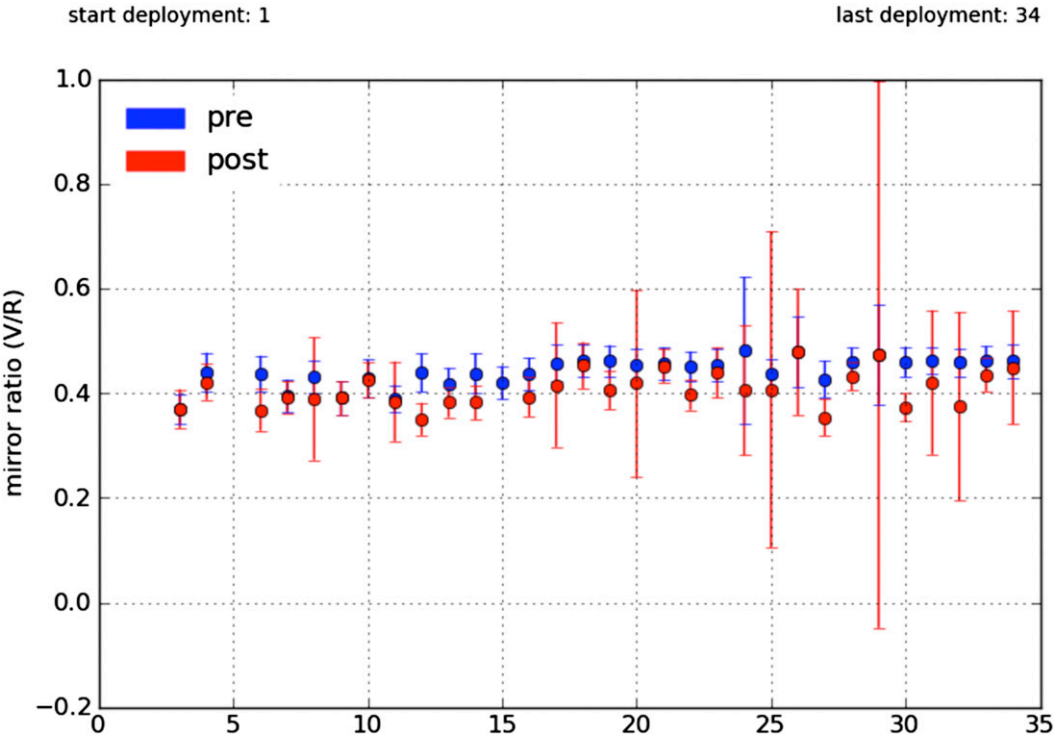

FIG. 10. ISAR-02 and ISAR-03 instrument-measured MR for 35 predeployment (blue) and postdeployment (red) calibration runs derived from CASOTS-II (serial 001) between 2004 and 2012. Dots represent the mean value of MR over the entire calibration run and error bars are the standard deviation of MR for that run.

tests are performed in a temperature-controlled room every 6 months. The room temperature is set at a given ambient temperature and a calibration using the CASOTS-II blackbody is performed. This is then repeated at other room temperatures to confirm that ISAR measurements are not adversely influenced by stray-light contamination. If needed, air conditioning is used to reduce the dewpoint temperature within the room to allow colder target temperatures to be achieved. Recent developments at the University of Miami (P. Minnett 2013, personal communication) allow radiometer laboratory calibration and validation work to be performed inside a tent that is flushed with dry air. This approach allows the reference blackbody temperatures to be set significantly below dewpoint temperatures without condensation forming on the inner walls of the reference blackbody.

The effort and investment required to maintain a rigorous and independent laboratory calibration history for all ISAR deployments is significant. However, as these data are used to validate costly satellite retrievals of SST (that are temporally and spatially extensive and therefore dominant compared to in situ SST measurements), this effort and investment is well justified. The CASOTS-II blackbody forms an essential element of the end-to-end validation activities performed by the ISAR program and the follow-on reporting of satellite SST uncertainties. ISAR data are approved for satellite validation analyses (e.g., Corlett et al. 2006; Wimmer et al. 2012) only if CASOTS-II pre- and postdeployment laboratory calibrations quantitatively demonstrate the same instrument accuracy of ±0.1 K. For a complete end-to-end validation of the at-sea measurement, a wide variety of sky radiance conditions, surface roughness conditions, ship movement, and their impact on estimates of seawater emissivity are required, which is beyond the scope of the laboratory work described here.

b. Using the CASOTS-II for ISAR development

Despite the extremely successful performance of ISAR when operated autonomously at sea, the ISAR scan mirror remains exposed to the external marine atmosphere during the measurement cycle and slowly degrades due to salt contamination over a period of ~(3–6) months. The ISAR internal calibration system accounts for a certain amount of contamination and corresponding increase in stray radiance as a consequence of an imperfect scan mirror surface. Nevertheless, an empirical approach to account for scan mirror degradation has been developed (Wimmer et al. 2012)

to improve data quality. The empirical coefficients of the adjustment procedure are derived using data obtained from the onboard calibration system of the ISAR radiometer but are verified using pre- and postdeployment CASOTS-II calibration verification data. Figure 10 shows the stability of the mirror ratio parameter MR, which is derived as the radiometric detector signal in volts (V) divided by the radiance (R) emitted from one of the onboard ISAR internal calibration blackbodies.

The quantity MR is found to be well defined and stable when validated using independent and fully characterized CASOTS-II data. If a scan mirror is contaminated, then the MR value is significantly depressed and has increased variability. The difference between the pre- and postdeployment MR values is used to define an empirical correction coefficient for stray-light corrections for that deployment run. Without the use of the CASOTS-II blackbody, mirror degradation adjustments to the final ISAR validation dataset could not be validated.

c. Using the CASOTS-II to identify and reject erroneous ISAR data

In 2006 the commercial manufacturing process of the ISAR scan mirror was modified. Some scan mirrors suffered serious degradation due to the saltwater atmosphere: the optical coating and gold surface blistered and was extensively corroded. In one case the mirror was so badly damaged that the ISAR data were unusable. Figure 11 shows the CASOTS-II calibration for this case obtained in January 2009. The CASOTS-II postdeployment calibration clearly identifies a damaged instrument. The CASOTS-II blackbody provided essential evidence to reject these data from further use. Furthermore, the data were subsequently used together with other calibration data to initiate discussions with the ISAR scan mirror manufacturer, leading to an improved mirror coating process that addresses the saline atmosphere mirror corrosion problem.

d. Using the CASOTS-II for ISAR instrument development

The ISAR radiometer has been developed over a 15-yr period during which it has undergone several significant design changes to the onboard electronics system, changes in suppliers of optical components, changes to component manufacturing processes, and upgrades to onboard and postprocessing software suites. The availability and use of the CASOTS-II blackbody has been fundamental to the evolution and development of the ISAR system in all of these cases. Furthermore, because multiple ISAR instruments are used within the AATSR satellite SST validation program, it has been extremely useful to quantify subtle differences between different instruments.

Figure 12 shows ISAR pre- and postdeployment calibration data for ISAR-02 and ISAR-03 instruments in cases where the postcalibration has used empirical stray radiance correction (Wimmer et al. 2012). The performance of the ISAR instruments over this period is shown to be consistent and stable with three notable exceptions. Deployments D15 and D26 were problematic, as the ISAR environmental protection shutter (see Donlon et al. 2009) had been damaged. The ISAR instrument could not obtain a postdeployment calibration without first rectifying this problem, resulting in a dataset that was not compliant with the requirement to perform both a pre- and postdeployment calibration. Six calibration runs of instrument ISAR-02 (D6, D8, D10, D12, D14, and D16) show a consistent −0.18 K bias with respect to other data. ISAR-02 at that time was using an older electronics package that had not been adequately matched to the onboard sensor components and their calibration coefficients. The CASOTS-II calibration data show the bias to be stable and recalibration corrections were successfully applied to all data until the electronics could be upgraded to address the issue at deployment 17. Several short (3–6 days) ISAR-02 deployments (D24, D26, and D29) were the first deployments of a new prototype electronics system and revealed significant deviations from the expected norms. While the calibration offset shown in Fig. 12 for these deployments could be corrected, the elevated noise for this particular instrument could not. These data were rejected and not used in any further analysis.

The data presented in Fig. 12 provide fundamental reference data that can be used by the ISAR engineering team to evolve and verify new instrument design; to identify, understand, and solve problems; and to maintain the high quality of the ISAR dataset when used for satellite validation work.

6. Protocols to maintain SI traceability of the shipborne ISAR radiometer for satellite SST validation

The protocols presented below are intended to guide any group collecting shipborne infrared radiometer data for use in satellite validation activities toward a ''common sense'' practice that will improve the quality and reduce the uncertainty in the satellite SST validation process. They are derived partly from the experience with CASOTS-II described in section 5, and from discussions with other pioneers of shipborne radiometry. Each individual deployment of a shipborne radiometer is highly specific, and the best practices noted below are a minimum requirement.

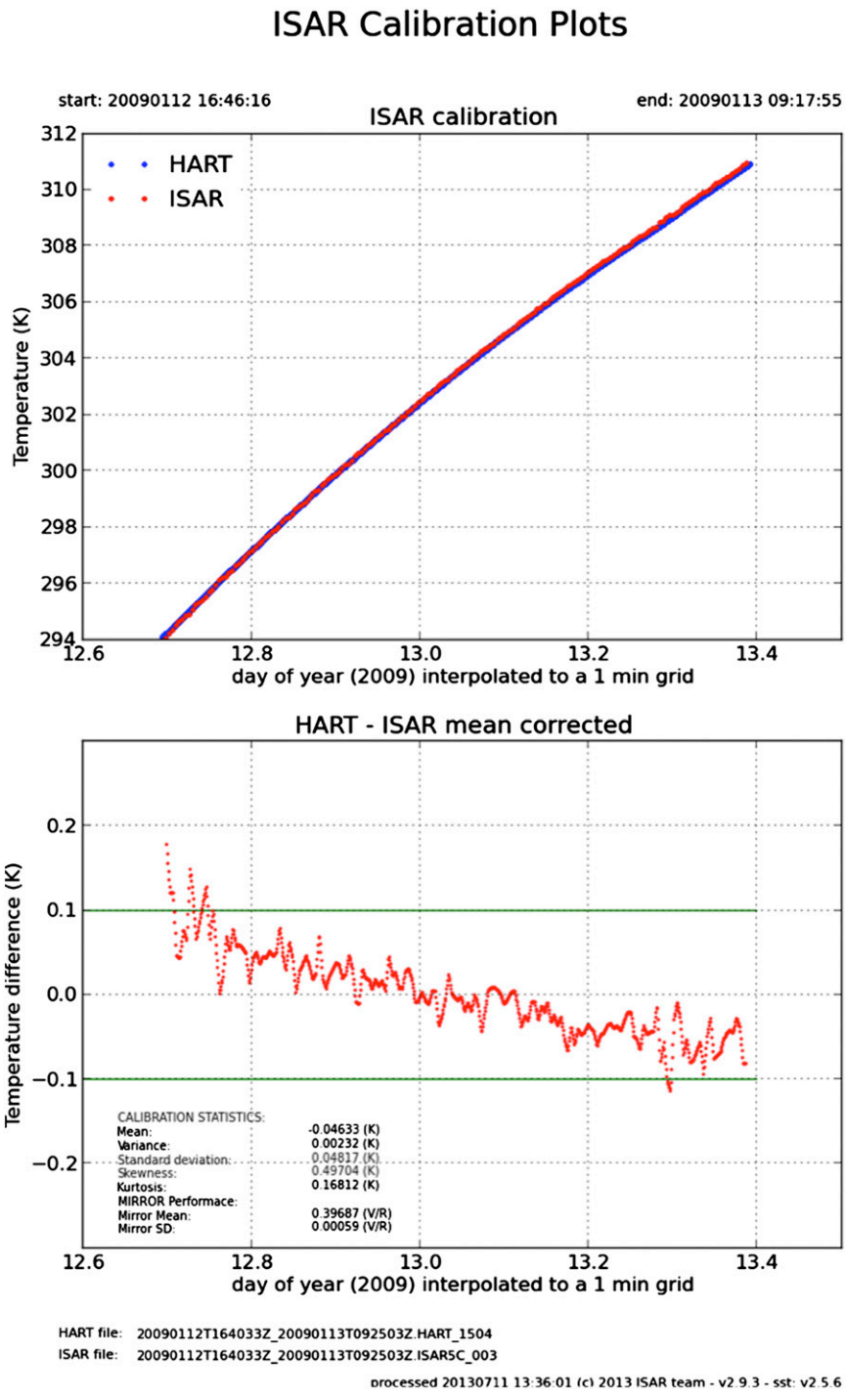

FIG. 11. As in Fig. 9, but for postdeployment after 3 months' operation in the Bay of Biscay, 12 Jan 2009.

a. Definition of measurement methodology

The exact methodology used to measure SST_{skin} using a shipborne radiometers shall be fully documented. This shall include the following:

- A full technical description of the radiometer instrument (spectral characteristics, sampling characteristics, measurement technique, a description of the instrument internal calibration approach, etc.)

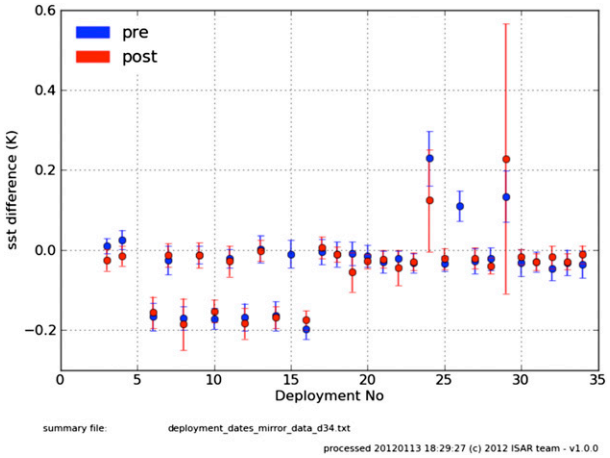

FIG. 12. Difference between ISAR-02 and ISAR-03 pre- and postdeployment for 35 calibration runs where the postcalibration has used an empirical stray radiance correction derived from CASOTS-II between 2004 and 2012. Dots represent the mean difference between ISAR and CASOTS-II temperatures computed at 1-min intervals over the entire calibration run and error bars are the standard deviation of the difference for that run. ISAR data have been postprocessed using the version 2.5.5 code.

- The spectral characteristics of the measurement system (i.e., instrument bandpass)
- The value used for seawater emissivity
- How the component of sky radiance reflected at the sea surface into the radiometer field of view is properly addressed (e.g., Donlon and Nightingale 2000)
- A description of the radiometer mounting arrangements and the geometric configuration of the radiometer with all measurement angles accurately documented
- A description of steps taken to ensure that measurements are free of ship effects (ship's bow wave, significant emission from the ship superstructure, emissions from ship exhaust plumes, etc.)
- Onboard instrument software used (version, release date, etc.)
- Data postprocessing software (version, release date, etc.)
- Any other aspect considered relevant to better understanding the quality of the measurements obtained.

b. *Definition of laboratory calibration and verification methodology and procedures*

Infrared radiometers typically used for satellite validation work are calibrated using onboard calibration reference radiance sources (blackbodies). The purpose of performing pre- and postdeployment verification using external reference blackbodies is to assess the accuracy of the internal calibration system, and to provide a link in an unbroken chain of comparisons linking the shipborne radiometer to an SI reference. The exact methodology and procedures used to perform a laboratory calibration and verification of a radiometer shall be defined and documented (for an example, see Theocharous and Fox 2010; Theocharous et al. 2010).

c. *Predeployment calibration verification*

Following the defined methodology and procedures set out under protocol 2, the calibration performance of a shipborne radiometer used for satellite product validation shall be verified prior to deployment using an external reference radiance source that is traceable to SI standards over the full range of sea surface temperatures expected for a deployment at sea. Ideally, the verification measurements should be repeated over a range of ambient temperatures to assess the influence of stray radiation on the radiometer measurements. The radiometer hardware, onboard configuration, onboard processing software, and data postprocessing software shall not be modified in any physical way between the calibration and the sea deployment (with the exception of dismounting and transporting the instrument to the calibration laboratory).

d. *Postdeployment calibration verification*

Following the defined methodology and procedures set out under protocols 2 and 3, the calibration performance of a shipborne radiometer used for satellite product validation shall be verified after deployment.

e. *Uncertainty budgets*

Shipborne radiometer calibration and verification data shall be linked to uncertainty budgets determined in agreement with defined National Standards Laboratory protocols (e.g., Bell 1999) accounting for a comprehensive range of uncertainty sources (contributions from instruments, processing, deployment restrictions, and environmental conditions, etc.; for e.g., see Theocharous and Fox 2010; Theocharous et al. 2010). An uncertainty budget for the end-to-end SST_{skin} measurement shall be provided.

f. *Improving traceability of calibration and verification measurements*

Efforts should be made where possible to define community consensus schemes and measurement protocols for calibration and verification. Well-documented data processing schemes and quality assurance criteria shall be established to ensure consistency and traceability to SI standards of in situ radiometer measurements used for satellite validation. Shipborne radiometer users must participate regularly in intercomparison ''round-robin'' tests and comparison with international standards to establish traceability for their data. We note the

importance of international radiometer and reference blackbody intercalibration experiments (e.g., Kannenburg 1998; Rice et al. 2004; Barton et al. 2004; Theocharous and Fox 2010; Theocharous et al. 2010; Minnett and Corlett 2012) under this protocol and stress the need for future activities of this type. They promote the dissemination of state-of-art knowledge on instrument calibration, measurement methods, data processing, training opportunities, and quality assurance.

g. Accessibility to documentation

Documentation describing the shipborne radiometer calibration and verification process shall be made available to the user community to promote peer review and ensure appropriate promulgation of knowledge on shipborne radiometer calibration and verification.

h. Archiving of data

Shipborne radiometer calibration and verification data should be archived following good data stewardship practices, providing access to records by research teams on request. Laboratory calibration and verification data shall be published in a format that is freely and openly available to users of the data.

i. Periodic consolidation and update of calibration and verification procedures

Shipborne radiometer calibration and verification measurement procedures should be consolidated as a result of a critical review of those currently documented in peer-review literature or already included in compilations produced by former programs and ''lessons learned'' from deployments aboard ships and in the laboratory. Consolidated protocols should be maintained and published. We note the potential of the GHRSST Satellite SST Validation (ST-VAL) group to act as a forum to consolidate and maintain international consensus under this protocol.

7. Summary and conclusions

A CASOTS-II blackbody system has been developed for use as an external reference blackbody for shipborne in situ radiometers. The CASOTS-II is designed to validate the internal calibration of and performance of ISAR radiometers to an accuracy of ±0.1K. The design follows the same overall system design principles as for the CASOTS-I system, providing a robust, low-cost, easy to manufacture and transport unit and offers the best compromise between portability and cost while maintaining the precision and accuracy required for producing SST_{skin} measurements from shipborne radiometer systems used for satellite validation activities. The worst-case standard uncertainty of the CASOTS-II blackbody for a measurement integration time of 20 s, a water bath temperature of 290 K, and 40-mm aperture (used by ISAR radiometers) is 16 mK, accounting for uncertainties of the thermometer and readout electronics, small temperature gradients across the cavity wall and paint, water bath heating rate, and thermal gradients in the water bath. In the worst case (using the full 110-mm aperture of the cavity), the radiance temperature of the CASOTS-II blackbody system is traceable to the SI with an uncertainty of 58 mK. This uncertainty was verified by an independent intercomparison with the U.K. National Physical Laboratory's AMBER radiometers and no significant differences were found within 75 mK (110-mm aperture) or 50 mK (40 mm aperture), the combined uncertainty of the comparison. This provides the reference standard for traceability of the ISAR SST_{skin} records used for satellite SST validation.

The CASOTS-II blackbody has been successfully used in laboratory calibrations of the University of Southampton's ISAR instruments for many years. The CASOTS-II underpins the use of the ISAR autonomous shipborne radiometer program that has proved to be effective in reliably measuring skin SST for satellite validation activities. Low (±0.1 K) ISAR instrument biases and standard deviation are independently confirmed using laboratory pre- and postdeployment calibration using the CASOTS-II system. CASOTS-II data allow quantitative uncertainty estimates to be assigned to each ISAR instrument and deployment dataset, improving confidence in these data compared to other SST validation datasets. The capacity of an autonomous shipborne radiometer to sustain extended 3-month high-quality deployments without the need for frequent operator intervention has been proven through the rigorous use of the CASOTS-II blackbody. Several hundred near-contemporaneous matchups between autonomous shipborne radiometers and satellite measurements are now a reality, allowing engineers and researchers to validate satellite products and to refine retrieval algorithms with confidence. The use of the CASOTS-II system has also allowed the ISAR team to diagnose and solve instrumental problems, develop new algorithms, diagnose component-manufacturing problems, and evolve the ISAR electronics system with confidence. The use of CASOTS-II or similar reference infrared radiance calibration sources provide an essential component of sustained satellite radiometer validation efforts for the present and future satellite instruments, such as the European Copernicus Sentinel-3 Sea and Land Surface Temperature Radiometer. In this context, shipborne radiometers following the measurement protocols described

in this paper provide a fiducial reference measurement (FRM) for satellite validation activities. Finally, as the CASOTS-II is traceable to SI standards, its use allows in situ shipborne radiometer data to be used with confidence as an independent validation for the SST climate data record.

Acknowledgments. The authors thank Prof. P. Minnett and the University of Miami for use of the ThermaCAM SC3000 thermal camera and their comments on the protocols presented in this paper. DEFRA and DECC funding supported a part of this work. The authors would like to thank two anonymous reviewers for their constructive review of the paper.

REFERENCES

Bahurel, P., and Coauthors, 2010: Ocean monitoring and forecasting core services, the European MyOcean example. *Proceedings of OceanObs'09: Sustained Ocean Observations and Information for Society,* J. Hall, D. E. Harrison, and D. Stammer, Eds., Vol. 1, ESA Publ. WPP-306, doi:10.5270/OceanObs09.pp.02.

Barton, I. J., P. J. Minnett, K. A. Maillet, C. J. Donlon, S. J. Hook, A. T. Jessup, and T. J. Nightingale, 2004: The Miami2001 infrared radiometer calibration and intercomparison. Part II: Shipboard results. *J. Atmos. Oceanic Technol.,* **21,** 268–283, doi:10.1175/1520-0426(2004)021<0268:TMIRCA>2.0.CO;2.

Bell, S., 1999: Measurement good practice guide: A beginner's guide to uncertainty of measurement. No. 11, Issue 2, 33 pp. [Available from National Physical Laboratory, Hampton Road, Teddington, Middlesex TW11 0LW, United Kingdom.]

Berry, K. H., 1981: Emissivity of a cylindrical black-body cavity with a re-entrant cone end face. *J. Phys.,* **14E,** 629, doi:10.1088/0022-3735/14/5/023.

Bras, B., 2013: Thermo-optical properties of NEXTEL velvet suede coating 3103 for Sentinel 3. ESA/ESTEC/TEC-QTE Rep. 7417, 16 pp. [Available from ESA/ESTEC, Keplerlaan 1, 2200 AG Noordwijk, Netherlands.]

Coll, C., E. Valor, J. M. Galve, M. Mira, M. Bisquert, V. García-Santos, E. Caselles, and V. Caselles, 2011: Long-term accuracy assessment of land surface temperatures derived from the Advanced Along-Track Scanning Radiometer. *Remote Sens. Environ.,* **116,** 211–225, http://dx.doi.org/10.1016/j.rse.2010.01.027.

Coppo, P., and Coauthors, 2010: SLSTR: A high accuracy dual scan temperature radiometer for sea and land surface monitoring from space. *J. Mod. Opt.,* **57,** 1815–1830, doi:10.1080/09500340.2010.503010.

Corlett, G. K., and Coauthors, 2006: The accuracy of SST retrievals from AATSR: An initial assessment through geophysical validation against in situ radiometers, buoys and other SST data sets. *Adv. Space Res.,* **37,** 764–769, doi:10.1016/j.asr.2005.09.037.

Donlon, C. J., and T. J. Nightingale, 2000: The effect of atmospheric radiance errors in radiometric sea surface temperature measurements. *Appl. Opt.,* **39,** 2387–2392, doi:10.1364/AO.39.002387.

——, ——, L. Fielder, G. Fisher, D. Baldwin, and I. S. Robinson, 1999: The calibration and intercalibration of sea-going infrared radiometer systems using a low cost blackbody cavity. *J. Atmos. Oceanic Technol.,* **16,** 1183–1192, doi:10.1175/1520-0426(1999)016<1183:TCAIOS>2.0.CO;2.

——, and Coauthors, 2007: The Global Ocean Data Assimilation Experiment High-Resolution Sea Surface Temperature Pilot Project. *Bull. Amer. Meteor. Soc.,* **88,** 1197–1213, doi:10.1175/BAMS-88-8-1197.

——, I. S. Robinson, M. Reynolds, W. Wimmer, G. Fisher, R. Edwards, and T. J. Nightingale, 2008: An Infrared Sea Surface Temperature Autonomous Radiometer (ISAR) for deployment aboard volunteer observing ships (VOS). *J. Atmos. Oceanic Technol.,* **25,** 93–113, doi:10.1175/2007JTECHO505.1.

——, and Coauthors, 2009: The GODAE High-Resolution Sea Surface Temperature Pilot Project (GHRSST-PP). *Oceanography,* **22,** 34–45, doi:10.5670/oceanog.2009.64.

——, and Coauthors, 2012: The Global Monitoring for Environment and Security (GMES) Sentinel-3 mission. *Remote Sens. Environ.,* **120,** 37–57, doi:10.1016/j.rse.2011.07.024.

Dybkjær, G., R. Tonboe, and J. Høyer, 2012: Arctic surface temperatures from Metop AVHRR compared to in situ ocean and land data. *Ocean Sci. Discuss.,* **9,** 1009–1043, doi:10.5194/osd-9-1009-2012.

Fowler, J. B., 1995: A third generation water bath based blackbody source. *J. Res. Natl. Inst. Stand. Technol.,* **100,** 591, doi:10.6028/jres.100.044.

——, 1996: An oil-bath-based 293 K to 473 K blackbody source. *J. Res. Natl. Inst. Stand. Technol.,* **101,** 629, doi:10.6028/jres.101.062.

GCOS-Secretariat, 2009: Guideline for the generation of satellite-based datasets and products meeting GCOS requirements. GCOS-128, WMO/TD-1488, 12 pp. [Available online at http://www.wmo.int/pages/prog/gcos/Publications/gcos-128.pdf.]

——, 2011: Systematic observation requirements for satellite-based products for climate: Supplemental details to the satellite-based component of the ''Implementation Plan for the Global Observing System for Climate in support of the UNFCCC (2010 update); 2011 update.'' GCOS 154, 127 pp. [Available online at http://www.wmo.int/pages/prog/gcos/Publications/gcos-154.pdf.]

Geist, J., and J. B. Fowler, 1986: A water bath blackbody for the 5 to 60°C temperature range: Performance goals, design concept, and test results. U.S. National Bureau of Standards and Technology Tech. Note 1228, 16 pp.

Guan, L., K. Zhang, and W. Teng, 2011: Shipboard measurements of skin SST in the China seas: Validation of satellite SST products. *2011 IEEE International Geoscience and Remote Sensing Symposium (IGARSS): Proceedings,* IEEE, 2005–2008, doi:10.1109/IGARSS.2011.6049522.

Jessup, A. T., R. Fogelberg, and P. Minnett, 2002: Autonomous shipboard infrared radiometer system for in situ validation of satellite SST. *Earth Observing Systems VII,* W. L. Barnes, Ed., International Society for Optical Engineering (SPIE Proceedings, Vol. 4814), 222, doi:10.1117/12.451782.

Kannenberg, R., 1998: IR instrument comparison workshop at the Rosenstiel School of Marine and Atmospheric Science (RSMAS). *The Earth Observer,* Vol. 10 (3), Earth Observing System Project Science Office, Greenbelt, MD, 51–54.

Legaie, D., H. Pron, C. Bissieux, and V. Blain, 2008: Thermographic application of black coatings on metals. Preprints, *Ninth Int. Conf. on Quantitative Infrared Thermography,* Krakow, Poland, Technical University of Lodz and AGH University of Science and Technology, 597–604. [Available online at http://qirt.gel.ulaval.ca/archives/qirt2008/papers/15_08_12.pdf.]

Lohrengel, R., and R. Todtenhaupt, 1996: Wämeleitfähigkeit, Gestamtemmissionsgrade und spektrale Emissionsgrade der

Beschichtung NEXTEL-Velvet-Coating 811-211 (RAL 900 15 teif-shwartz matt). *PTB-Mitt.,* **106,** 259–265.

Mason, I. M., P. H. Sheather, J. A. Bowles, and G. Davies, 1996: Blackbody calibration sources of high accuracy for a spaceborne infrared instrument: The Along Track Scanning Radiometer. *Appl. Opt.,* **35,** 629–639, doi:10.1364/AO.35.000629.

McKelvie, J., 1987: Consideration of the surface temperature response to cyclic thermoelastic heat generation. *Stress Analysis by Thermoelastic Techniques,* B. C. Gasper, Ed., International Society for Optical Engineering (SPIE Proceedings, Vol. 731), 44, doi:10.1117/12.937886.

Meldrum, D., E. Charpantier, M. Fedak, B. Lee, R. Lumpkin, P. Niller, and H. Viola, 2010: Data buoy observations: The status quo and anticipated developments over the next decade. *Proceedings of OceanObs'09: Sustained Ocean Observations and Information for Society,* J. Hall, D. E. Harrison, and D. Stammer, Eds., Vol. 2, ESA Publ. WPP-306, doi:10.5270/OceanObs09.cwp.62.

Merchant, C. J., and Coauthors, 2012: A 20 year independent record of sea surface temperature for climate from Along-Track Scanning Radiometers. *J. Geophys. Res.,* **117,** C12013, doi:10.1029/2012JC008400.

Minnett, P. J., 2010: The validation of sea surface temperature retrievals from spaceborne infrared radiometers. *Oceanography from Space, Revisited,* V. Barale, J. F. R. Gower, and L. Alberotanza, Eds., Springer Science and Business Media, 229–248, doi:10.1007/978-90-481-8681-5.

——, and G. K. Corlett, 2012: A pathway to generating climate data records of sea-surface temperature from satellite measurements. *Deep-Sea Res. II,* **77–80,** 44–51, doi:10.1016/j.dsr2.2012.04.003.

——, R. O. Knuteson, F. A. Best, B. J. Osborne, J. A. Hanafin, and O. B. Brown, 2001: The Marine–Atmospheric Emitted Radiance Interferometer: A high-accuracy seagoing infrared spectroradiometer. *J. Atmos. Oceanic Technol.,* **18,** 994–1013, doi:10.1175/1520-0426(2001)018<0994:TMAERI>2.0.CO;2.

Noyes, E. J., P. J. Minnett, J. J. Remedios, G. K. Corlett, S. A. Good, and D. T. Llewellyn-Jones, 2006: The accuracy of the AATSR sea surface temperatures in the Caribbean. *Remote Sens. Environ.,* **101,** 38–51, doi:10.1016/j.rse.2005.11.011.

Persky, M. J., 1999: Review of black surfaces for space-borne infrared systems. *Rev. Sci. Instrum.,* **70,** 2193–2217, doi:10.1063/1.1149739.

QA4EO Task Team, 2010: A quality assurance framework for Earth observation: Principles, version 4. Group on Earth Observations, 17 pp. [Available online at http://qa4eo.org/docs/QA4EO_Principles_v4.0.pdf.]

Rice, J., and Coauthors, 2004: The Miami2001 infrared radiometer calibration and intercomparison. Part I: Laboratory characterization of blackbody targets. *J. Atmos. Oceanic Technol.,* **21,** 258–267, doi:10.1175/1520-0426(2004)021<0258:TMIRCA>2.0.CO;2.

Robinson, A. F., J. M. Dulieu-Barton, S. Quinn, and R. L. Burguete, 2010: Paint coating characterization for thermoelastic stress analysis of metallic materials. *Meas. Sci. Technol.,* **21,** 085502, doi:10.1088/0957-0233/21/8/085502.

Sea-Bird Electronics, Inc., 2011: SBE 38 digital oceanographic thermometer user's manual. Version 13, 03-23-11, 33 pp. [Available from Sea-Bird Electronics, Inc., 13431 NE 20th Street, Bellevue, WA 98005.]

Theocharous, E., and N. P. Fox, 2010: CEOS comparison of IR brightness temperature measurements in support of satellite validation. Part II: Laboratory comparison of the brightness temperature of blackbodies, National Physical Laboratory Rep. OP-4, 43 pp.

——, ——, V. I. Sapritsky, S. N. Mekhontsev, and S. P. Morozova, 1998: Absolute measurements of black-body emitted radiance. *Metrologia,* **35,** 549, doi:10.1088/0026-1394/35/4/58.

——, E. Usadi, and N. P. Fox, 2010: CEOS comparison of IR brightness temperature measurements in support of satellite validation. Part I: Laboratory and ocean surface temperature comparison of radiation thermometers, National Physical Laboratory Rep. OP-3, 130 pp.

Wimmer, W., I. Robinson, and C. Donlon, 2012: Long-term validation of AATSR SST data products using shipborne radiometry in the Bay of Biscay and English Channel. *Remote Sens. Environ.,* **116,** 17–31, doi:10.1016/j.rse.2011.03.022.